

國立交通大學

電信工程學系

碩士論文

進階性無線網路媒介存取控制與路由協
定技術

Advanced Medium Access Control and
Routing Techniques for Wireless
Networks

研究生：黃瑜智

指導教授：方凱田

中華民國 97 年 6 月

國立交通大學

電信工程學系

碩士論文

進階性無線網路媒介存取控制與路由協
定技術



Advanced Medium Access Control and
Routing Techniques for Wireless
Networks

研究生：黃瑜智

指導教授：方凱田

中華民國 97 年 6 月

進階性無線網路媒介存取控制與路由協定技術

Advanced Medium Access Control and Routing Techniques for
Wireless Networks

研究生：黃瑜智

Student：Yu-Tzu Huang

指導教授：方凱田

Advisor：Kai-Ten Feng

國立交通大學

電信工程學系碩士班



A Thesis

Submitted to Department of Communication Engineering
College of Electrical and Computer Engineering
National Chiao Tung University
in Partial Fulfillment of the Requirements
for the Degree of
Mater of Science
in Communication Engineering
June 2008
Hsinchu, Taiwan, Republic of China

中華民國 97 年 6 月

進階性無線網路媒介存取控制與路由協定技術

學生：黃瑜智

指導教授：方凱田

國立交通大學電信工程學系碩士班

摘 要

由於近年無線區域網路技術的興起，使得提高單位時間內有效的資料傳輸量成為很重要的議題。IEEE 802.11n 中，訊框堆合為改善整體傳輸效率技術之一。為了使訊框堆合能有效使用於非理想傳輸通道中，錯誤重傳機制提供了可靠傳輸的解決辦法。在此篇論文中，針對選擇性訊框重傳以及混合式選擇性訊框重傳配合訊框堆合技術進行效能分析。混合式選擇性訊框重傳技術，利用直接錯誤更正技術，將發生錯誤之訊框直接更正，進而降低重傳訊框時所耗費的時間並提高了有效傳輸資料量。結果我們可以發現，當處於雜訊環境中，混合式選擇性訊框重傳機制配合訊框堆合技術，可以達到大幅提高有效資料傳輸量的目的。論文的第二部份，針對無線網路中的群播協定進行研究與設計。當處於無線環境中，由於群播協定中常需要轉傳點以傳送資料至特定群組成員。而相同的資料封包，常存在有多餘的轉傳點傳送。若以省能點觀點角度思考，如何節省轉傳點的數量為實際面臨的問題，此篇論文對此問題提出試誤性的解決辦法，並實際利用嵌入式平臺作為演算法設計之系統。

Advanced Medium Access Control and Routing Techniques for Wireless Networks

Student : Yu-Tzu Huang

Advisor : Kai-Ten Feng

Department of Communication Engineering
National Chiao Tung University

Abstract

The next generation wireless local networks (WLANs) with enhanced throughput performance have attracted significant amounts of attention in recent years. Based on the IEEE 802.11n standard, frame aggregation is considered one of the major factors to improve the system performance of WLANs from the medium access control (MAC) perspective. In order to fulfill the requirements of the high-throughput performance, feasible design of automatic retransmission request (ARQ) mechanisms is considered important for providing reliable data transmission. However, none of the existing retransmission schemes is specifically designed under high throughput requirements. In this paper, two ARQ schemes are proposed to consider the effect from frame aggregation for the enhancement of network throughput. An aggregated selective repeat ARQ (ASR-ARQ) algorithm is proposed, which incorporate the selective repeat ARQ scheme with the consideration of frame aggregation. On the other hand, the aggregated hybrid ARQ (AH-ARQ) mechanism is proposed to further enhance the throughput performance by adapting the forward error correction (FEC) scheme. The proposed AH-ARQ algorithm is considered as a MAC-defined retransmission scheme by exploiting the Reed- Solomon block code.

The analytical models for both the ASR-ARQ and the AH-ARQ algorithms are established in this paper, where the scenarios with and without interfering stations are analyzed. Simulations are also conducted to validated and compare the proposed ARQ mechanisms with other existing schemes based on the service time distribution. It will be shown in the numerical evaluation that the proposed AH-ARQ algorithm outperforms the other retransmission schemes owing to its effective utilization of the FEC mechanism.

In the second part of this paper, we focus the topic on the implementation and design of a multicast routing protocol. It is known that how to provide low energy consumption and high

packet delivery ratio are considered the major issues in the protocol design for the wireless multihop networks. The main focus of this part is to reduce the number of data transmissions such that the energy consumption can be decreased. In the wired networks, the Steiner-Tree is regarded as an optimal approach to construct the multicast structure for specific senders and receivers. However, it is considered an NP-Hard problem for achieving the minimum cost multicast tree under the wireless broadcast environment.

In this paper, an Energy-Conserving Multicast Routing (ECMR) protocol is proposed as a heuristic scheme to reduce the number of relaying nodes for the construction of the multicast mesh. Moreover, the proposed algorithm is implemented on an ARM-based embedded platform for performance evaluation. Comparing with the existing multicast routing protocol, the experimental results show that the proposed ECMR scheme can provide better energy conservation while the packet delivery ratio is still preserved.



誌謝

兩年的研究所生活在本論文完成的同時，也畫上了句點。首先要感謝指導教授方凱田老師，在研究的過程中提供許多的建議，固定的討論讓自己的構思能夠更完備，也從實驗室定期的報告訓練中獲益良多。同時感謝交通大學電子系黃經堯教授和資工系趙禧綠教授，撥空來參加口試並給予很多實質的建議，使得論文更趨完整。

感謝給予我無代價支持的家人，分享生活中的喜更分享生活中的苦，家人讓我知道永遠都會有人在支持我。感謝實驗室的學長學弟們，仲賢、昭霖、文炫、文俊、裕彬、育群、柏軒、信龍、林志、柏泰。你們的陪伴和支持讓我有勇氣繼續往人生下個階段挑戰，你們的肯定和教導讓我知道自己的無限可能。

黃瑜智 謹誌 于交通大學 2008/06

Contents

Chinese Abstract	I
English Abstract	II
Foreword	IV
Contents	V
List of Figures	VIII
<i>I Performance Analysis of MAC Defined Hybrid ARQ Scheme for Next Generation Wireless Networks</i>	
1 Introduction	2
2 Proposed Automatic Retransmission reQuest Mechanisms	5
2.1 Frame Aggregation/De-aggregation of IEEE 802.11n MAC Protocol	5
2.2 Proposed Aggregated Selective Repeat (ASR) ARQ Scheme	7
2.3 Proposed Aggregated Hybrid (AH) ARQ Scheme	8
2.3.1 FEC Mechanism of AH-ARQ Scheme	8
2.3.2 Retransmission Mechanism of the AH-ARQ Scheme	11
3 System Models	13
3.1 Queuing Model of Frame Aggregation	13
3.2 Service Models	14
4 Unsaturated Performance Analysis of Proposed ARQ Schemes	17

4.1	Modeling of Service Time Distribution of Proposed ASR-ARQ Scheme	
		17
4.2	Modeling of Service Time Distribution of Proposed AH-ARQ Scheme	
		22
4.3	Iteration Algorithm for Proposed ARQ Schemes	25
5	Performance Analysis of Proposed ARQ Schemes with Existence of Interfering Stations	26
5.1	Modeling of Service Time Distribution of Proposed ASR-ARQ Scheme with Contending Stations	26
5.2	Modeling of Service Time Distribution of Proposed AH-ARQ Scheme with Contending Stations	29
6	Performance Evaluation	33
7	Conclusion	42
	Bibliography	43
	<i>II Efficient Implementation of an Energy-Conserving Multicast Routing Protocol for Wireless Multihop Networks</i>	46
8	Introduction	47
9	The Proposed Energy-Conserving Multicast Routing (ECMR) Protocol	49
9.1	The Concept of Heuristic Structure Construction	49
9.2	The Pseudo Code of Heuristic Structure Construction	50
9.3	Data Packet Forwarding	53
10	Performance Evaluation	54
10.1	The Software and Hardware Architectures	54



10.2	The Experiment Results	56
11	Conclusion	59
Bibliography		60



List of Figures

2.1 Frame aggregation: (a) A-MPDU frame format, (b) Modified MPDU format for AH-ARQ.	6
2.2 Flow diagram for the MS to process the incoming A-MPDU, where N denotes the number of RS codewords within a MPDU.	10
2.3 Flow diagram of the retransmission mechanism of the AH-ARQ scheme	12
3.1 Markov chain for service time models.	15
4.1 Signal flow graph of the specified Markov chain with initial state N.	18
5.1 Service System Diagram.	28
6.1 (a) Cumulated Density Function versus Number of Retransmission Stages with ASR mechanism. The A-MPDU consists of 10 MPDUs. (b) Cumulated Density Function versus Number of Retransmission Stages with AHR mechanism. Each MPDU consists of 3 RS Blocks.	36
6.2 An aggregated frame consists of 10 MPDUs for AH-ARQ (AHR) and ASR-ARQ(ASR). For pure aggregated MSDU mechanism (AMS), there are same number(10) of MSDUs within a MPDU. The information payload is 657- byte-long	

within a MPDU in ASR and ASR schemes. For AMS, the MSDU consists of 657 bytes information payload. (a) Normalized MAC Throughput, (b) Mean Service Time. 37

6.3 An aggregated frame consists of 50 MPDU_s for AH-ARQ (AHR) and ASR-ARQ(ASR). For pure aggregated MSDU mechanism (AMS), there are same number(50) of MSDUs within a MPDU. The information payload is 657- byte-long within a MPDU in ASR and ASR schemes. For AMS, the MSDU consists of 657 bytes information payload. (a) Normalized MAC Throughput, (b) Mean Service Time. 38

6.4 MAC Service Time Distribution of AH-ARQ under $BER = 10^{-2}$; $[\alpha, \beta] = [5, 10]$, unsaturation case with five iterations. Number of RS blocks = 3, and each RS block consists of 219-byte-long information octets. 39

6.5 MAC Service Time Distribution of ASR-ARQ under $BER = 2 \times 10^{-4}$; $[\alpha, \beta] = [5, 10]$, unsaturation case with five iterations. Each MPDU consists of 657-byte-long information payload. 39

6.6 Cumulated Density Function of ASR-ARQ Scheme under $BER = 2 \times 10^{-4}$, saturation case. NoS = 3, and each MPDU consists of 657-byte-long information payload. 40

6.7 Cumulated Density Function of ASR-ARQ Scheme under $BER = 2.5 \times 10^{-4}$, saturation case. NoS = 3, and each MPDU consists of 657-byte-long information payload. 40

6.8 Cumulated Density Function of AHR-ARQ Scheme under $BER = 10^{-2}$, saturation case. NoS = 3, number of RS blocks = 3, and each RS block consists of

219-byte-long information octets. 41

6.9 Cumulated Density Function of AHR-ARQ Scheme under $BER = 1.1 \times 10^{-2}$, saturation case. NoS = 3, number of RS blocks = 3, and each RS block consists of 219-byte-long information octets. 41

10.1 Left: the software and hardware architectures for the proposed ECMR protocol; Right: the snapshot of the PCM-7230 ARM-based embedded platform 55

10.2 The network topology for field experiments: the source node S communicates with three receivers R_1 , R_2 , and R_3 via the intermediate nodes I_1 and I_2 . The solid lines denote the connectivity between the corresponding two nodes. 56

10.3 (a) Energy Consumption for Relaying Data Packets vs. Round Index, (b) Packet Delivery Ratio vs. Packet Inter-Departure Time. 58



Part I

Performance Analysis of MAC Defined

Hybrid ARQ Scheme for Next Generation Wireless Networks



Chapter 1

Introduction

In recent years, the techniques for wireless local area networks (WLANs) have been prevailing exploited for both indoor and mobile communications. The applications for WLANs include point-to-point bridges and ad-hoc networking. Among different techniques, the IEEE 802.11 standard is the considered the well-adopted suite due to its remarkable success in both design and deployment.

Various amendments are contained in the IEEE 802.11 standard suite, mainly including IEEE 802.11a/b/g , IEEE 802.11e for quality-of-service (QoS) support, and the IEEE 802.11n [1] [2] [3] for high throughput performance. The simplicity of the carrier sense multiple access with collision avoidance (CSMA/CA) scheme for the medium access control (MAC) has contributed to the success of the IEEE 802.11 specifications. The WLAN devices that implement the IEEE 802.11b Physical (PHY) layer support the data transmission rate of 11 Mbps; while the data rate of the IEEE 802.11a PHY technique can sustain up to 54 Mbps with the adoption of the orthogonal frequency-division multiplexing (OFDM) transmission scheme. Moreover, there are increasing demands for high throughput communication devices in order to support multimedia applications, e.g. HDTV and DVD. In order to fulfill the requirement for achieving improved throughput performance, the IEEE 802.11 task group N (TGn) enhances the PHY layer data rate to 600 Mbps by adopting advanced communication techniques, such as multi-input multi-output (MIMO) technology [4]. It is noted that MIMO technique utilizes spatial diversity to improve both the range and spatial multiplexing for achieving higher data rate. However, it has been investigated in [5] that simply improves the PHY data rate will not be suf-

for enhancing the system throughput from the MAC perspective. Accordingly, the IEEE 802.11 TGn further exploits frame aggregation and block acknowledgement techniques [6] to moderate the drawbacks that are originated from the MAC/PHY overheads.

Although the frame aggregation can reduce both the transmission time for frame headers and the contention time induced by the random back-off period, a larger aggregated frame will cause each station to wait for an elongated period before the next chance for channel access. Furthermore, under the error-prone channels, corrupting an aggregated frame can result in the wastage of a longer period of channel time and consequently lead to a lowered MAC throughput. As a result, a feasible design of the retransmission mechanisms becomes a significant topic with the existence of the frame aggregation scheme.

The automatic retransmission request (ARQ) [7] [8] [9] mechanisms have been extensively proposed in different wireless systems for reliable transmission. In order to reach more reliable transmissions within a shorter delivery period, the hybrid ARQ (H-ARQ) schemes [10] [11], which combine both the forward error correction (FEC) and the retransmission mechanism, have been proposed for advanced multimedia applications. In general, the H-ARQ mechanisms can be classified into three categories. In the type-I H-ARQ scheme [12], as a error packet is detected via the cyclic redundancy check, the transmitter will retransmit the same packet either until the packet is successfully decoded at the receiver or a maximum retransmission limit is reached. Type-II of H-ARQ scheme is regarded as the full incremental redundancy(IR) technique [13], which decreases the coding rate in each retransmission by sending additional redundancy check digits. On the other hand, type-III of H-ARQ scheme [14], considered as a partial IR scheme, not only decrements the coding rate but also maintains the self-decoding capability in each retransmission. It is noted that the IR-based schemes in general make use of the rate compatible punctured convolutional (RCPC) codes [14] [15] or the rate compatible punctured turbo (RCPT) codes. Moreover, the transmission errors are in general corrected in two phases based on the design concept of the concatenate code [16]. The inner decoder, which is implemented in the PHY layer, adopts sophisticated algorithms for error correction; while the outer decoder is served as the second stage fine-tuning error corrector that is operated in the MAC layer protocols. As a consequence, the FEC scheme in type-II and III of H-ARQ algorithms is regarded as

the inner decoder; while that of type-I scheme is considered as the outer decoder.

However, none of the existing ARQ algorithms are specifically designed under the scenarios with frame aggregation. It is require to provide an efficient retransmission scheme such as to enhance the system throughput for the IEEE 802.11n networks. In this paper, two ARQ schemes are proposed to consider the effect from frame aggregation in order to improve the network throughput. An aggregated selective repeat ARQ (ASR-ARQ) algorithm is proposed, which incorporate the selective repeat ARQ scheme with the consideration of frame aggregation. On the other hand, the aggregated hybrid ARQ (AH-ARQ) mechanism is proposed to further enhance the throughput performance for the IEEE 802.11n networks. It is considered as a Type-I of H-ARQ algorithm, which can be served as a outer code designed from the MAC layer perspective. The Reed-Solomon (RS) code [17] [18], which defines finite codeword length, is adopted within the proposed AH-ARQ scheme. Furthermore, it will be beneficial to construct effective analytical models to evaluate of the retransmission mechanisms for the IEEE 802.11n networks. There are existing studies propose analytical models for performance evaluation of the MAC channel access [19] [20] [21] and the frame aggregation techniques [22] [23] [24] for the IEEE 802.11-based networks. However, none of these models considers efficient retransmission schemes that are especially feasible for the high throughput required environments. As a result, the analytical models for both the ASR-ARQ and the AH-ARQ algorithms are established in this paper, where the scenarios with and without the collision probability are considered. Simulations are also conducted to validated and compare the proposed ARQ schemes based on the service time distribution. It will be shown in the numerical evaluation that the AH-ARQ algorithm outperform the other schemes owing to its efficient utilization of the FEC mechanism.

The remainder of the first part is organized as follows. chapter 2 describes the conventional and newly defined MAC mechanism for 802.11n. The proposed analytical model for MAC mechanisms are in chapter 2, 3, and 4. Chapter 5 provides the performance evaluation and chapter 6 draws the conclusions.

Chapter 2

Proposed Automatic Retransmission reQuest Mechanisms

2.1 Frame Aggregation/De-aggregation of IEEE 802.11n MAC Protocol

The IEEE 802.11n standard mandates the implementation of frame aggregation scheme for the sake of promoting the transmission efficiency. It is noted that the transmission efficiency is defined as the time for delivering the information payload over the time durations for transmitting the entire aggregated frame associated with the required control packets and the contention period. With frame aggregation scheme as shown in Fig. 2.1(a), multiple MAC protocol data units (MPDUs) are combined into an aggregated MPDU (A-MPDU), which is consequently transported into a single PHY service data unit (PSDU). Intuitively, the transmission efficiency can be improved with the utilization of the A-MPDU since more MPDUs are transmitted with a communion of control overhead.

Each MPDU is padded with a MPDU delimiter for the purpose of extracting the corresponding MPDU from the aggregated frame. The extracting delimiter is composed of four bytes as shown in Fig. 2.1(a), including the reserved, MPDU length, CRC, and the unique pattern (UP) fields. It is noted that the UP field, which is set to the ASCII value of character 'N', is employed to detect a MPDU delimiter while scanning within the aggregation. Moreover, each MPDU is padded to become a multiple of 4 octets as shown in Fig. 2.1(a). The de-aggregation procedure at the receiver side that

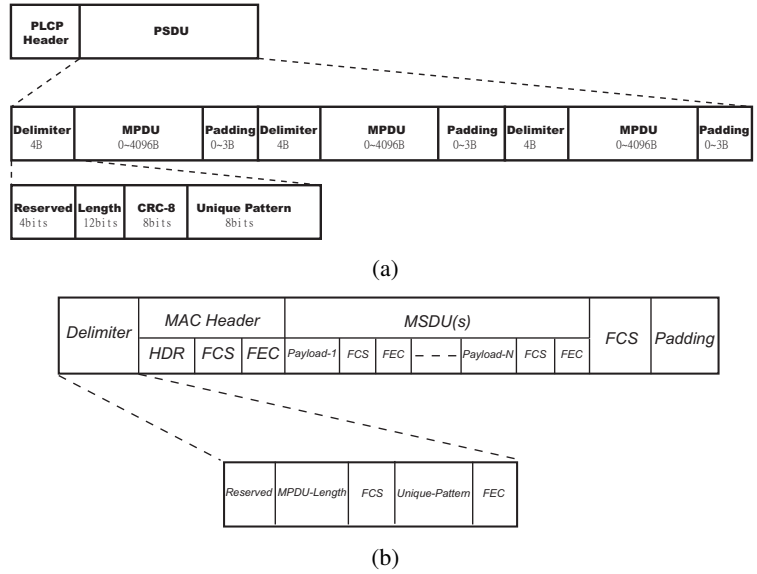


Figure 2.1: Frame aggregation: (a) A-MPDU frame format, (b) Modified MPDU format for AH-ARQ.

was described in the standard is rewritten into pseudo-code as shown in Algorithm 1. The receiver verifies the validity of the MPDU delimiter via the `valid_MPDU_Delimiter` function (in Algorithm 1) based on the 8-bits CRC and the observation of the UP field, i.e. with character 'N'. The MPDU will be successfully extracted from the aggregate if the MPDU delimiter is found to be valid. On other other hand, the de-aggregation process will move forward with four bytes (i.e. the offset parameter in Algorithm 1) and continue to verify if the next multiple of four octets contains a valid delimiter.

Algorithm 1: De-aggregation Process for an A-MPDU

```

offset = 0 ;
while offset+4 ≤ A_MPDU_length do
    length = get_MPDU_length(offset) ;
    if [valid_MPDU_delimiter(offset)] = True & [0 < length ≤
    Max_MPDU_length] = True then
        Receive_MPDU(offset+4,length) ;
        offset = offset + 4 * [(length + 4)/4] ;
    else
        offset = offset + 4 ;

```

2.2 Proposed Aggregated Selective Repeat (ASR) ARQ Scheme

The design of retransmission mechanisms is considered an open topic from the standpoint of the IEEE 802.11n standard. In this paper, the proposed ASR-ARQ scheme is modified from the conventional selective repeat (SR) ARQ mechanism to consider the packet aggregation within the design of retransmission mechanism. Contributing from the availability of the block acknowledgement (BA) scheme within the IEEE 802.11n standard, the ASR-ARQ algorithm can be effectively designed to provide transmission efficiency. Instead of sending each MPDU within an A-MPDU, the receiver replies with a BA frame for acknowledging the entire A-MPDU that is initiated from the transmitter. The BA frame consists of 32 octets which contains a bitmap field. Each bit in the bitmap field identifies whether the corresponding MPDU from the aggregated frame has been correctly received. As a consequence, the single BA frame reduces the control overhead comparing with conventional design by sending multiple ACK frames for an aggregated data frame.

In the proposed ASR-ARQ scheme, each MPDU is identified via a unique sequence number while an aggregated frame is transmitted. In the case that some of the MPDUs within an A-MPDU are missing during the transmission, the ASR-ARQ algorithm will continue to retransmit those unsuccessfully transmitted MPDUs until all the MPDUs have either been positively acknowledged by the BA frame or reach the retry limitation. For instance, there are N MPDUs contained within an A-MPDU that are identified by the sequence numbers from 1 to N . If the MPDUs with sequence numbers 3 and 5 are corrupted and are identified via CRC check, the receiver will reply with the BA frame which denotes two zero flags at the corresponding third and fifth bits within the bitmap field. A new aggregated frame, which includes only the third and fifth MPDUs, will be delivered by the transmitter at the next transmission opportunity. The retransmission procedure terminates until either all the MPDUs with sequence numbers from 1 to N are correctly accepted by the receiver or the maximum number of retransmission trials (i.e. identified by the `Retry_Limit` parameter) has achieved.

2.3 Proposed Aggregated Hybrid (AH) ARQ Scheme

In order to further enhance the transmission efficiency, the AH-ARQ scheme is proposed to integrate both the RS-based FEC and the retransmission mechanisms. Both the FEC and the retransmission schemes are described in the next two subsections.

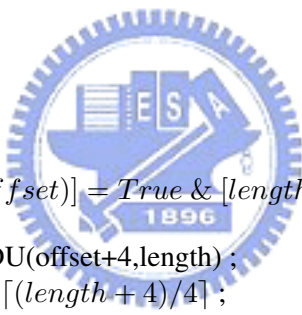
2.3.1 FEC Mechanism of AH-ARQ Scheme

Based on the existing IEEE 802.11n MAC frame structure, the proposed FEC mechanism is constructed according to the RS code that are well-adopted in the design of outer decoders. The coefficients of the generator polynomial $G(x)$ are elements in a finite field $GF(2^m)$, where $m = 8$ is chosen according to the byte-oriented system. For a (n, k, τ) RS code, the set of roots $\alpha = \{\alpha, \alpha^2, \dots, \alpha^{2\tau}\}$ of $G(x)$ are selected from the $GF(2^8)$, where α is a primitive element of the finite field. As a result, the generator polynomial $G(x)$ can be represented as $G(x) = \prod_{k=1}^{2\tau} (x + \alpha^k) = x^{2\tau} + \sum_{i=0}^{2\tau-1} g_i x^i$. Based on the cyclic property of the RS code, the set of codewords can be formed with the multiplication of both the $G(x)$ and the information symbols polynomial $I(x)$. Moreover, the RS code will have the minimum codeword distance $d_{min} \geq 2\tau + 1$ in the case that all the coefficients g_i (for all $i \in \{0, \dots, 2\tau - 1\}$) are not equal to zero. Therefore, the corresponding RS code possesses the correcting capability of τ error symbols associated with the codeword length of $2^8 - 1 = 255$ octets and k information octets. There are total of $n - k = 2\tau$ parity check octets, which are served as the remainder $R(x)$ while dividing $x^{2\tau} I(x)$ by the generator polynomial $G(x)$. In order to extract the newly defined MPDU that includes the FEC mechanism, a modified de-aggregation procedure is performed as shown in Algorithm 2. At the beginning, the scanning process will start to search for the UP. After the UP has been identified, an additional predefined symbol will be traversed for verifying the usage of the FEC scheme. In other words, a valid delimiter will be identified if the recovered reserved field within the delimiter matches the ASCII value of character FF. It is noted that other functionalities can be referred as in Algorithm 1 in the similar manner.

After the de-aggregation process has been defined, the entire mechanism for the MS to manage the incoming A-MPDU is explained as follows (as in Fig. 2.2). The MS will first start to extract each MPDU within an A-MPDU based on Algorithm 2. In the case that the MS has successfully

Algorithm 2: FEC-enhanced De-aggregation Process for an A-MPDU

```
offset = 0 ;
while  $offset + 4 + 2t \leq A\_MPDU\_length$  do
  length = get_MPDU_length(offset) ;
  if Succ_Dec_Delimiter(offset, offset + 4) then
    if [valid_fcs_check(offset)] = True & [get_reserved_bits(offset) = FF] =
      True & [length ≤ Max_MPDU_length] = True then
      RS_Dec_MPDU(offset+4+2t,length);
      offset = offset + 4 · ⌈(4 + 2t + length)/4⌉ ;
    end
  else
    offset = offset + 4;
  end
end
else
  if [valid_fcs_check(offset)] = True & [length ≤ Max_MPDU_length] = True
  then
    Normal_Recv_MPDU(offset+4,length) ;
    offset = offset + 4 · ⌈(length + 4)/4⌉ ;
  end
  else
    offset = offset + 4;
  end
end
end
```



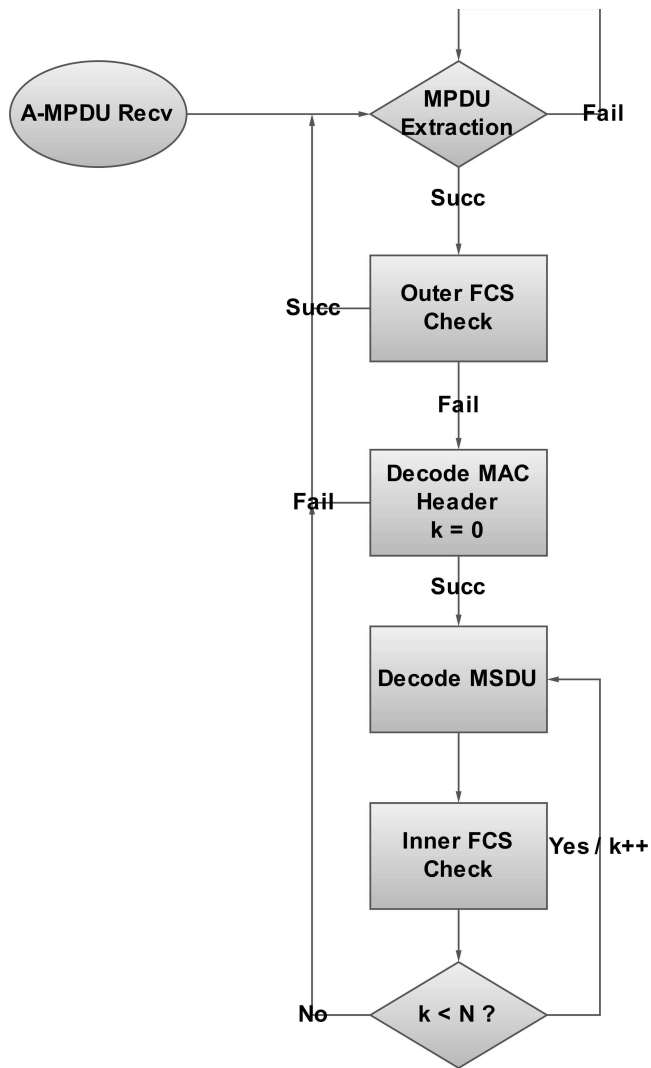


Figure 2.2: Flow diagram for the MS to process the incoming A-MPDU, where N denotes the number of RS codewords within a MPDU.

extracts an MPDU and observing that the corresponding outer FCS is correct, the MS will enable the corresponding bits within the bitmap field of the BA frame. On the other hand, if the outer FCS of the corresponding MPDU is incorrect, the MS will execute the RS decoder in order to decode the RS block in the MAC header. It is noted that the well-adopted Berlekamp's iterative algorithm is adopted to implement the decoding procedure. If either the decoding process fails or the invalid inner FCS of the MAC header RS block occurs, the process will be terminated with disabling the corresponding bits within bitmap field of BA frame. On the other hand, if the MS successfully decodes the MAC header RS block, it will continue to decode the entire MPDU via the RS decoder. The MS will set the corresponding bits within the bitmap field of the BA frame according to the above results. As a result, the MS will send a BA frame back to the AP if it has successfully extracted each MPDU from the A-MPDU.

2.3.2 Retransmission Mechanism of the AH-ARQ Scheme

The flow diagram for the retransmission mechanism of the proposed AH-ARQ scheme is depicted in Fig. 2.3. It is noted that the main concept of the retransmission scheme is to implement the conventional ASR-ARQ scheme on the codeword basis. The receiver will store the correctable RS block and combines these blocks with remaining retrieved correctable RS blocks in order to form a complete new frame. The detail mechanism is explained as follows. Initially, the transmitter starts by transmitting an A-MPDU with M MPDUs and $M \times N$ RS blocks to the receiver. After receiving the A-MPDU, the receiver will extract each MPDU with the adoption of Algorithm 2. The receiver finds errors within a set of RS blocks that are correctable, it will enable the corresponding bits within bitmap field of BA frame. On the other hand, if these RS blocks are uncorrectable, the receiver disables the corresponding bits of the MPDU within bitmap field of BA frame. The receiver will store the set of correctly received RS blocks of the MPDU and the associated header information, i.e. both the sequence number and the retried times of this MPDU. The receiver will consequently send a BA frame back to the transmitter if all the MPDUs of an A-MPDU have been extracted. The transmitter retransmits an A-MPDU with each MPDU containing both the MAC header RS block and other uncorrectable RS blocks in ascending sequence.

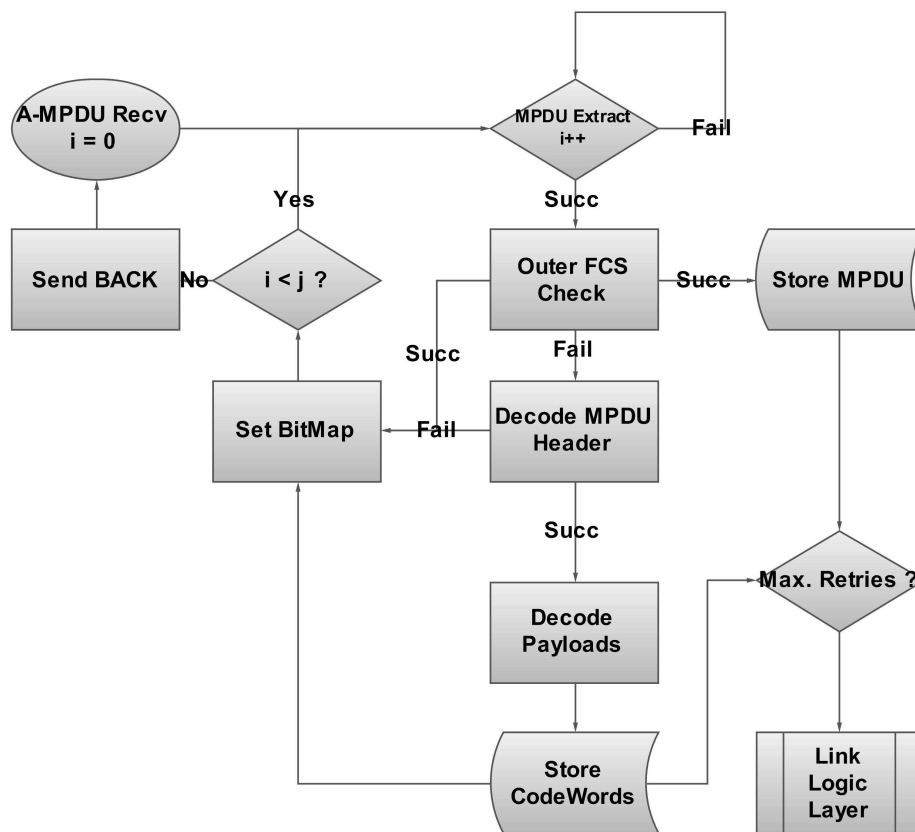


Figure 2.3: Flow diagram of the retransmission mechanism of the AH-ARQ scheme

Chapter 3

System Models

In this section, the required system models for the design of the proposed ARQ schemes are explained. Section 3.1 describes the queuing model for the 802.11n MAC protocol under the unsaturated situation. The service models based on the Markovian chain are presented in Section 3.2.

3.1 Queuing Model of Frame Aggregation

In order to describe the traffic characteristics of the 802.11n MAC protocol for the unsaturated case, a discrete time $M/G^{[\alpha,\beta]}/1/K$ queuing model is adopted in this paper. It is noted that $[\alpha, \beta]$ denotes the integer range for the total number of aggregated packets, and K is the maximum number of packets that can be stored in the queue. An imbedded Markov process ξ_n is considered at the time instant δ_n^- just before the departure of the aggregated packets. The discrete form of $\xi(\delta_n^-)$ can be represented by the state space $\mathcal{S} = \{S_j | j \in \mathbb{N}, 0 \leq j \leq K\}$, where S_j denotes that there are j packets waiting in the queue; while the transition probability can be defined as $p_{ij}^{(m)} = Prob.\{\xi(\delta_n^-) = S_j | \xi(\delta_{n-m}^-) = S_i\}$. From the properties of ergodic Markov chains, the convergence of transition probability is obtained as $\lim_{m \rightarrow \infty} p_{ij}^{(m)} = p_{ij}$. The steady state probabilities are represented as $\pi_j = \lim_{m \rightarrow \infty} \pi_j^{(m)} = \lim_{m \rightarrow \infty} \sum_i \pi_i^{(0)} \cdot p_{ij}^{(m)} = \sum_i \pi_i^{(0)} \cdot p_{ij}$. Considering the case with unlimited queue length (i.e.

$K \rightarrow \infty$), the steady state probabilities π_j can be obtained as

$$\pi_j = \begin{cases} k_0 \sum_{i=0}^{\beta} \pi_i, & \text{for } j = 0 \\ \sum_{i=0}^{\beta} k_j \cdot \pi_i + \sum_{i=\beta+1}^{\beta+j} k_{\beta+j-i} \cdot \pi_i, & \text{for } j \geq 1 \end{cases} \quad (3.1)$$

where $k_j = \int_0^{\infty} e^{-\lambda t} \frac{(\lambda t)^j}{j!} dT(t)$. $T(t)$ represents the cumulative distribution function (CDF) of service time distribution for medium access delay, and λ indicates the packet arrival rate. On the other hand, considering the case with limited queue length K , the steady state probabilities π_j as in (3.1) can be modified as

$$\pi_j = \begin{cases} k_0 \sum_{i=0}^{\beta} \pi_i, & j = 0 \\ \sum_{i=0}^{\beta} k_j \cdot \pi_i + \sum_{i=\beta+1}^{\beta+j} k_{\beta+j-i} \cdot \pi_i, & 1 \leq j < K - \beta \\ \sum_{i=0}^{\beta} k_j \cdot \pi_i + \sum_{i=\beta+1}^K k_{\beta+j-i} \cdot \pi_i, & K - \beta \leq j < K \\ 1 - \sum_{i=0}^{K-1} \pi_i, & j = K \\ 0, & j > K \end{cases} \quad (3.2)$$

It is noted that the queuing model with limited queue length (as in (3.2)) will be utilized in chapter 5 for the derivation of unsaturated performance of the proposed ARQ schemes.

3.2 Service Models

As shown in Fig. 3.1, the state probability $b_{i,j}$ for the AP can be derived from the Markov-Chain model. It is noted that $b_{i,0} = p_{i-1,f} \cdot b_{i-1,0}$, where $b_{i,j}$ denotes the state probability identified by the (i, j) pair and $p_{i-1,f}$ represents the failed transmission probability at the $(i-1)$ th stage. It is noted that $p_{i-1,f}$ will be acquired in the latter subsections based on the different proposed schemes. Therefore, the state probability $b_{i,j}$ can be inferred as

$$b_{i,j} = \sum_{k=j}^{2^i W - 1} b_{i-1,0} \cdot \frac{p_{i-1,f}^k}{2^{iW}} = \left(1 - \frac{j}{2^{iW}}\right) b_{i-1,0} \cdot p_{i-1,f}^j \quad (3.3)$$

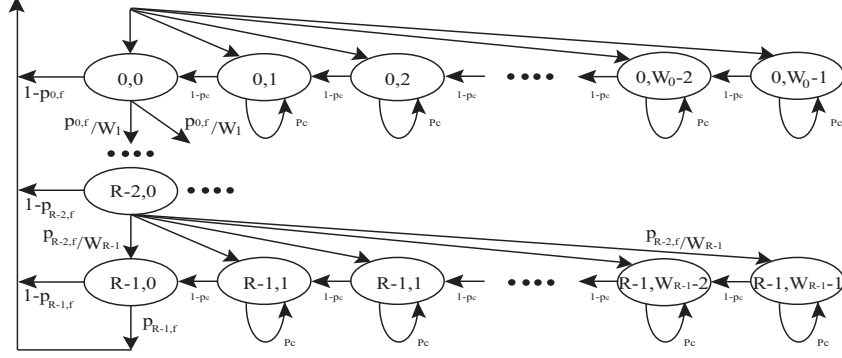


Figure 3.1: Markov chain for service time models.

where W indicates the minimum contention window size. Based on (3.3) and $b_{i,0} = \prod_{j=0}^{i-1} p_{j,f} \cdot b_{0,0}$, the probability that the MAC service is busy can be obtained as

$$P_{busy} = \sum_{i=0}^{R-1} \sum_{j=0}^{2^i W - 1} b_{i,j} = \sum_{i=0}^{R-1} \frac{b_{0,0} (2^{\frac{|i+M|-|i-M|}{2}} W + 1)}{2} \prod_{k=0}^{i-1} p_{k,f} \quad (3.4)$$

where R indicates the retry limit and M denotes the maximum number of retransmissions. Therefore, the maximum contention window size becomes $2^M W$. Consequently, the transmitting probability τ condition on that the MAC is busy becomes

$$\tau = \frac{\sum_{i=0}^{R-1} b_{i,0}}{P_{busy}} = \frac{1 + \sum_{i=1}^{R-1} \prod_{k=0}^{i-1} p_{k,f}}{\frac{W+1}{2} + \sum_{i=1}^{R-1} \frac{(2^{\frac{|i+M|-|i-M|}{2}} W + 1)}{2} \prod_{k=0}^{i-1} p_{k,f}} \quad (3.5)$$

On the other hand, the service model with collision probability p_c not equals zero is considered and derived. The Markov Chain model as in Fig. (3.1) is also adopted in this case. Similar to (3.3),

the state probability $b_{i,j}$ for the case that $p_c \neq 0$ can be inferred as

$$b_{i,j} = \begin{cases} b_{i-1,0} \cdot p_{i-1,f}, & j = 0 \\ p_{i-1,f} \cdot \left(1 - \frac{j}{2^i W}\right) \cdot \frac{b_{i-1,0}}{1-p_c}, & 1 \leq j < 2^i W - 1 \end{cases} \quad (3.6)$$

for $1 \leq i < R$. Based on (3.6) and $b_{i,0} = b_{0,0} \prod_{m=0}^{i-1} p_{m,f}$, the transmitting probability τ , collision probability p_c , and successful transmission probability p_s can be obtained as

$$\tau = \frac{1 + \sum_{i=1}^{R-1} \prod_{m=0}^{i-1} p_{m,f}}{1 + \frac{W-1}{2(1-p_c)} + \sum_{i=1}^{R-1} \left[1 + \frac{2^{\lfloor \frac{M+i}{2} \rfloor - \lfloor \frac{M-i}{2} \rfloor} (W-1)}{2(1-p_c)}\right] \prod_{m=0}^{i-1} p_{m,f}} \quad (3.7)$$

$$p_c = 1 - (1 - \tau)^{N-1} \quad (3.8)$$

$$p_s = (N - 1)\tau(1 - \tau)^{N-2} \quad (3.9)$$

where N denotes the total number of contenting stations.



Chapter 4

Unsaturated Performance Analysis of Proposed ARQ Schemes

In this chapter, the performance modeling of the proposed ASR-ARQ and AH-ARQ mechanisms are established under the unsaturated situation; while limited queue with queue length is equal to K is considered. A pair of transmitter and receiver with either up-link or down-link unicast transmission is considered for performance analysis. Furthermore, the distributed coordination function (DCF) is employed as the medium access scheme for one access category between the transmitter and the receiver. The request-to-send/clear-to-send (RTS/CTS) mechanism is used for channel reservation for enhancing basic access mechanism. The packet size of the incoming MAC service data units (MSDUs) are assumed fixed. The performance analysis for both the proposed ASR-ARQ and AH-ARQ schemes are explained in Sections 4.1 and 4.2. The iterative algorithm for conducting the ARQ schemes are presented in Section 4.3.

4.1 Modeling of Service Time Distribution of Proposed ASR-ARQ Scheme

The service time distribution for the transmitter can be obtained from the state diagram based on the modified Bianchi's model [19]. As stated in the IEEE 802.11n standard, the time duration for long NAV (T_{LNAV}) should be long enough to accommodate a typical A-MPDU sequence. In general, T_{LNAV} is suggested to be twice in time duration compared with the time required for the A-MPDUs

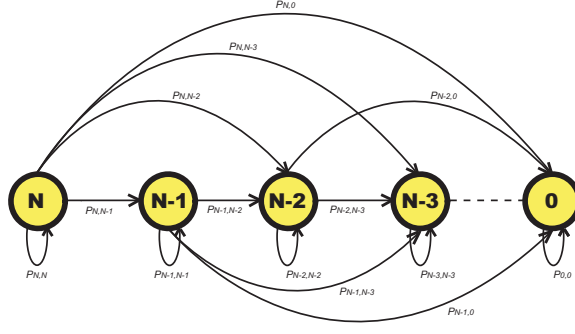


Figure 4.1: Signal flow graph of the specified Markov chain with initial state N.

transmission, i.e. $T_{LNAV} = T_{RTS} + T_{CTS} + 2T_{A-MPDU} + 2T_{BA} + 5T_{SIFS}$. The second A-MPDU time duration is occupied only if the first A-MPDU is failed in transmission. In order to calculate the probability mass function of random variable which denotes the required times such that all the MPDUs have been positive acknowledged based on the proposed ASR-ARQ scheme, the signal flow graph of the specified Markov chain is depicted as in Fig. 4.1. The recurrent relationship $F_j(D)$ can be formulated as

$$F_j(D) = \begin{cases} 1, & \text{for } j=1 \\ \sum_{k=0}^j \sum_{m=0}^k C_k^j C_m^k (1-p_{f,e})^{j-m} p_{f,e}^{k+m} D F_m(D), & \text{for } j > 1 \end{cases} \quad (4.1)$$

where D represents the transition gain as the state changes, and $p_{f,e}$ denotes the frame error probability. In order to solve the recurrent equation as in (4.1), the transformed function $\tilde{F}(x)$ is defined as

$$\tilde{F}(x) \triangleq \sum_{j=0}^{\infty} F_j(D) \frac{x^j}{j!}. \quad (4.2)$$

By substituting x in (4.2) with $p_{f,e}^2 x$ associated with the relationships $e^{(1-p_{f,e})x} = \sum_{j=0}^{\infty} \frac{[(1-p_{f,e})x]^j}{j!}$ and $e^{(1-p_{f,e}^2)x} = \sum_{j=0}^{\infty} \frac{[(1-p_{f,e}^2)x]^j}{j!}$, $\tilde{F}(x)$ can be acquired as

$$\tilde{F}(x) = D \tilde{F}(p_{f,e}^2 x) e^{(1-p_{f,e}^2)x} + (1-D). \quad (4.3)$$

By defining $Q(x) \triangleq \frac{\tilde{F}(x)}{e^x}$, (4.3) can be rewritten as

$$Q(x) = Q(p_{f,e}^2 x)D + (1 - D)e^{-x} \quad (4.4)$$

On the other hand, $Q(x)$ can be written as

$$Q(x) = \sum_{j=0}^{\infty} Q_j(D) \frac{x^j}{j!} \quad (4.5)$$

By incorporating (4.4) and (4.5), $Q(x)$ can be obtained as

$$Q(x) = \sum_{j=0}^{\infty} \left[D \frac{(p_{f,e}^2 x)^j}{j!} Q_j(D) + (-1)^j (1 - D) \frac{x^j}{j!} \right]. \quad (4.6)$$

which can further be rewritten as

$$Q_j(D) = \frac{(-1)^j (1 - D)}{1 - D p_{f,e}^{2j}}. \quad (4.7)$$

By substituting (4.7) into (4.5), $\tilde{F}(x)$ can be rewritten as

$$\tilde{F}(x) = e^x Q(x) = \left[\sum_{j=0}^{\infty} \frac{(-1)^j (1 - D)}{1 - D p_{f,e}^{2j}} \frac{x^j}{j!} \right] \cdot \sum_{k=0}^{\infty} \frac{x^k}{k!}. \quad (4.8)$$

Finally, $F_j(D)$ can be obtained from (4.2) and (4.8) as

$$F_j(D) = \sum_{k=0}^j \frac{j!}{(j-k)!k!} \frac{(-1)^k (1 - D)}{1 - D p_{f,e}^{2k}}. \quad (4.9)$$

The recurrent function $F_j(D)$ as in (4.9) implies the mechanism of the SR-ARQ scheme, which will also later be utilized for the computation of the failed transmission probability $p_{m,f}$.

Moreover, it is noticed that the medium access delay can be divided into two parts, including the back-off delay and the transmission delay. First of all, the back-off delay is represented by considering the probability generating function (PGF) of consecutive back-off time slots $H_d(z)$, which is defined as $H_d(z) = z^\sigma$ with σ denoting the length of a single time slot. Accordingly, the PGF for the back-off

delay at the i th back-off stage $H_i(z)$ is obtained as

$$H_i(z) = \begin{cases} \frac{1}{2^i W} \sum_{k=0}^{2^i W - 1} H_d^k(z), & 0 \leq i < M \\ \frac{1}{2^M W} \sum_{k=0}^{2^M W - 1} H_d^k(z), & M \leq i \leq R - 1 \end{cases} \quad (4.10)$$

On the other hand, the transmission delay is composed by both the unsuccessful and the successful transmission time. The conditional PGF $E_{m,f}^j(z)$ by considering the unsuccessful transmission between the m th and the $(m + 1)$ th back-off stages can be written as

$$E_{m,f}^j(z) = \sum_{j=\alpha}^{\beta} \frac{p_j}{1 - p_{m,0}^j} \sum_{k=1}^j \frac{p_{m,k}^j}{p_{s,k}} \sum_{i=1}^k C_i^k p_{f,e}^i (1 - p_{f,e})^{k-i} z^{T_{RTS} + T_{CTS} + 3T_{SIFS} + k\eta + T_{BA}} \sum_{l=1}^i C_l^i p_{f,e}^l (1 - p_{f,e})^{i-l} z^{i\eta + 2T_{SIFS} + T_{BA}} \quad (4.11)$$

where $p_{s,k} = 1 - \sum_{v=0}^k C_v^k p_{f,e}^v (1 - p_{f,e})^k$. It is noted that $E_{m,f}^j(z)$ corresponds to the PGF of the failed transmission time at the m th stage, where j denotes that there are j MPDUs initially aggregated. The parameter η in (4.11) is acquired as $\eta = (N_d \times T_s) / B(m)$, where N_d represents the number of data bytes per MPDU, T_s corresponds to the symbol duration, and $B(m)$ indicates the number of data bytes per OFDM symbol in the transmission mode m with one spatial stream. The distribution of aggregated p_j can be obtained as

$$p_j = \begin{cases} \sum_{i=0}^{\alpha} \pi_i, & j = \alpha \\ \pi_j, & \alpha < j < \beta \\ \sum_{i=\beta}^K \pi_i, & j = \beta \end{cases} \quad (4.12)$$

where π_j s are obtained from (3.2) in chapter IV under the case of limited queue length. The parameter $p_{m,k}^j$ denotes the probability that there are k unsuccessfully transmitted MPDUs, which can be represented as the $(k + 1)$ th element of the vector $v_p^{(m)}$, i.e. $p_{m,k}^j = [v_p^{(m)}]_{1,k+1}$. It is noticed that $v_p^{(m)} = v_p^{(0)} \times \mathbf{P}^{2m}$, which corresponds to the multiplication of the initial vector $v_p^{(0)} = [0 \ 0 \ \dots \ 0 \ 1]$ and the transition matrix \mathbf{P}^{2m} . It can be obtained that the elements within $\mathbf{P}_{(j+1) \times (j+1)}$ can be acquired

as

$$p_{i,j} = \begin{cases} 1, & i = j = 0 \\ C_j^i p_{f,e}^j (1 - p_{f,e})^{i-j}, & i \geq j \\ 0, & i < j \end{cases} \quad (4.13)$$

Furthermore, the probability $p_{m,0}^j$ within (4.11) can be obtained from the recursion equation (4.9) as

$$p_{m,0}^j = \sum_{k=1}^m \frac{d^k F_j(D)}{k! d D^k} \quad (4.14)$$

Moreover, the conditional PGF $S_n^j(z)$ of the j initially aggregated packets in service for the successful transmission time at the n -th back-off stage is obtained as

$$S_n^j(z) = \sum_{j=\alpha}^{\beta} \frac{p_j}{1 - p_{n,0}^j} \sum_{k=1}^j \frac{p_{n,k}^j}{p_{\epsilon,k}} [(1 - p_{f,e})^k z^{T_{RTS} + T_{CTS} + 3T_{SIFS} + k\eta + T_{BA}} + \sum_{i=1}^k C_i^k p_{f,e}^i (1 - p_{f,e})^k z^{T_{RTS} + T_{CTS} + 5T_{SIFS} + (k+i)\eta + 2T_{BA}}] \quad (4.15)$$

where $p_{\epsilon,k} = 1 - \sum_{l=1}^k \sum_{r=1}^l C_l^k C_r^l p_{f,e}^{l+r} (1 - p_{f,e})^{k-r}$. As a consequence, the overall PGF $T(z)$ of the MAC access time distribution can be formulated by combining (4.10), (4.11), and (4.15) as

$$T(z) = (1 - p_{0,f}) z^{T_{DIFS}} H_0(z) S_0(z) + \left\{ \sum_{i=1}^{R-1} \left[\prod_{j=0}^i z^{T_{DIFS}} H_j(z) \right] \left[\prod_{m=0}^{i-1} p_{m,f} E_{m,f}(z) \right] \right\} (1 - p_{i,f}) S_i(z) + \prod_{i=0}^{R-1} z^{T_{DIFS}} H_i(z) \prod_{m=0}^{R-1} p_{m,f} E_{m,f}(z) \quad (4.16)$$

where the failed transmission probability $p_{m,f}$ at m -th stage could be calculated as

$$p_{m,f} = \sum_{j=\alpha}^{\beta} p_j \sum_{k=1}^j p_{m,k}^j p_{s,k}$$

4.2 Modeling of Service Time Distribution of Proposed AH-ARQ Scheme

In this section, the performance analysis and modeling of the service time distribution of the proposed AH-ARQ scheme is presented. Based on the RS code, it is assumed that the decoding errors will occur while there are more than t corrupted symbols within a predefined block. Therefore, a decoding error probability $P_{block,e}$ of a block can be formulated as

$$P_{block,e} = \sum_{i=t+1}^n C_k^n p_{s,e}^k (1 - p_{s,e})^{n-k} \quad (4.17)$$

where $n = 2^m - 1$ represents the codeword length. It is noted that $p_{s,e}$ represents the error rate of an RS symbol defined in $GF(2^m)$ with m bits, i.e. $p_{s,e} = 1 - (1 - p_{b,e})^m$ where $p_{b,e}$ corresponds to the bit error rate. As a result, the recurrent relationship defined for transmitting A-MPDUs in one LNAV channel reservation duration could be reformulated as

$$F_i(D) = \begin{cases} 1, & i = 0 \\ P_e^2 D F_i(D) + 2P_e(1 - P_e) D \sum_{k=0}^i C_k^i P_{block,e}^k (1 - P_{block,e})^{i-k} F_k(D) + \\ (1 - P_e)^2 D \sum_{k=0}^i \sum_{l=0}^k C_k^i C_l^k P_{block,e}^{k+l} (1 - P_{block,e})^{i-l} F_l(D), & 1 \leq i \leq N \end{cases} \quad (4.18)$$

where N denotes the number of codewords in an MPDU and P_e represents the union of the error probabilities from both the packet header and the delimiter, i.e. $P_e = p_{hdr,e} \cup p_{delimiter,e} = p_{hdr,e} + p_{delimiter,e} - p_{hdr,e} \cdot p_{delimiter,e}$. It is noticed that if the value of P_e is greater than 0, the entire MPDU will be retransmitted. In order to represent the case for a MPDU that is composed of N RS blocks under error-prone channels, similar procedures as in (4.2) - (4.9) are adopted for solving the recurrent relationship. The recurrent function $F_i(D)$ can be acquired as

$$F_i(D) = \sum_{k=0}^i \frac{i!}{(i-k)!k!} \frac{(D-1)(-1)^k}{2DP_e(1-P_e)P_{block,e}^k + D(1-P_e)^2P_{block,e}^{2k} - (1-DP_e^2)} \quad (4.19)$$

for $1 \leq i \leq N$. Consequently, an MPDU consists of N RS blocks with retransmission mechanism under error-prone channel is depicted. It is noted that the recurrent function $F_i(D)$ obtained from (4.19) is merely considered for a single MPDU. The case with j MPDUs that are aggregated in one frame

is considered as follows. A discrete random variable X is considered which indicates the number of retried transmissions until all the RS blocks of an A-MPDU have been positive acknowledged. The probability density function (PDF) of X can be represented as

$$P_X(x) = \left[\sum_{i=1}^x \frac{1}{i!} \frac{d^i F_N(D)}{dD^i} \right]^j u(x) - \left[\sum_{i=1}^{x-1} \frac{1}{i!} \frac{d^i F_N(D)}{dD^i} \right]^j u(x-1) \quad (4.20)$$

In order to calculate the service time distribution of the proposed AH-ARQ scheme, both the PGFs for the failed transmission $E_{m,f}^j(z)$ and successful transmission $S_{m,f}^j(z)$ are to be acquired. The transfer function of the failed transmission time $E_{m,f}^j(z)$ at m th back-off stage is formulated as

$$\begin{aligned} E_{m,f}^j(z) \simeq & \sum_{k=1}^N \frac{p_{m,k}^N}{(1-p_{m,0}^N) p_{s,k}^{(FEC)}} \left[P_e^2 z^{2t_{oh}+2k\eta+\frac{2T_{BA}+3T_{SIFS}}{j}} + \right. \\ & (1-P_e) P_e \sum_{i=1}^k C_i^k P_{block,e}^i (1-P_{block,e})^{k-i} z^{2t_{oh}+(k+i)\eta+\frac{2T_{BA}+3T_{SIFS}}{j}} + \\ & (1-P_e) P_e \sum_{i=1}^k C_i^k P_{block,e}^i (1-P_{block,e})^{k-i} z^{2t_{oh}+2k\eta+\frac{2T_{BA}+3T_{SIFS}}{j}} + \\ & \left. (1-P_e)^2 \sum_{i=1}^k \sum_{l=1}^i C_i^k C_l^i (1-P_{block,e})^{k-l} P_{block,e}^{i+l} z^{2t_{oh}+(k+i)\eta+\frac{2T_{BA}+3T_{SIFS}}{j}} \right] z^{\frac{T_{RTS}+T_{CTS}+2T_{SIFS}}{j}} \end{aligned} \quad (4.21)$$

where $p_{s,k}^{(FEC)} = 1 - (1-P_e)(1-P_{block,e})^k - P_e(1-P_e)(1-P_{block,e})^k - (1-P_e)^2 \sum_{i=1}^k C_i^k P_{block,e}^i (1-P_{block,e})^k$. It is noted that the approximation is resulted from the case that the communion of time intervals for control packets. $k\eta$ represents the time interval for each RS block transmission; while t_{oh} corresponds to the time for k codewords to share one MAC header. The parameter $p_{m,k}^j$ represents the probability that there are k unsuccessfully received RS blocks after m retransmissions, which can be represented as the $(k+1)$ th element of the vector $v_p^{(m)}$, i.e. $p_{m,k}^j = [v_p^{(m)}]_{1,k+1}$. It is noticed that $v_p^{(m)} = v_p^{(0)} \times \mathbf{T}^{2m}$, which corresponds to the multiplication of the initial vector $v_p^{(0)} = [0 \ 0 \ \dots \ 0 \ 1]$ and the transition matrix \mathbf{T} for each transmission opportunity. It can be obtained that the elements

within $\mathbf{T}_{(N+1) \times (N+1)}$ can be acquired as

$$t_{i,j} = \begin{cases} 1, & i = j = 0 \\ P_e + (1 - P_e)P_{block,e}^i, & 1 \leq i \leq N, j = i \\ C_j^i (1 - P_e)P_{block,e}^j (1 - P_{block,e})^{i-j}, & 0 \leq j < i \\ 0, & i < j \end{cases} \quad (4.22)$$

And from eqn. (4.20),

$$P_X(x) = (p_{x,0}^N)^j u(x) - (p_{x-1,0}^N)^j u(x-1). \quad (4.23)$$

Consequently, $p_{m,0}^N$ can be derived. Furthermore, the successful transmission time between stage m and stage $m+1$ is depicted as

$$\begin{aligned} S_m^j(z) \simeq & \sum_{k=1}^N \frac{p_{m,k}^N}{(1 - p_{m,0}^N) p_{\epsilon,k}^{(FEC)}} [(1 - P_e)(1 - P_{block,e})^k z^{t_{oh} + k\eta + \frac{T_{SIFS} + T_{BA}}{j}} + \\ & P_e(1 - P_e)(1 - P_{block,e})^k z^{2t_{oh} + 2k\eta + \frac{3T_{SIFS} + 2T_{BA}}{j}} + \\ & (1 - P_e)^2 \sum_{l=1}^k C_l^k P_{block,e}^l (1 - P_{block,e})^k z^{2t_{oh} + (k+l)\eta + \frac{3T_{SIFS} + 2T_{BA}}{j}}] z^{\frac{T_{RTS} + T_{CTS} + 2T_{SIFS}}{j}} \end{aligned} \quad (4.24)$$

where $p_{\epsilon,k}^{(FEC)} = 1 - P_e^2 - 2(1 - P_e)P_e \sum_{i=1}^k C_i^k P_{block,e}^i (1 - P_{block,e})^{k-i} - (1 - P_e)^2 \sum_{i=1}^k \sum_{l=1}^i C_i^k C_l^i P_{block,e}^{i+l} (1 - P_{block,e})^{k-l}$. Therefore, the PGF of the service time distribution for a single MPDU can be obtained as

$$T(z) \simeq (1 - p_{0,f}) z^{T_{DIFS}} H_0(z^{j^{-1}}) S_0^j(z) + \sum_{i=1}^{R-1} (1 - p_{i,f}) \quad (4.25)$$

$$\left[\left(\prod_{l=0}^i z^{T_{DIFS}} H_l(z^{j^{-1}}) \right) \left(\prod_{m=0}^{i-1} p_{m,f}^{(FEC)} E_{m,f}^j(z) \right) \right] S_i^j(z) + \prod_{i=0}^{R-1} z^{T_{DIFS}} H_i(z^{j^{-1}}) \prod_{m=0}^{R-1} p_{m,f} E_{m,f}^j(z). \quad (4.26)$$

where $p_{m,f}^{(FEC)}$ represents the failed transmission probability for an MPDU containing N RS blocks, i.e. $p_{m,f} = \sum_{k=1}^N p_{m,k}^N p_{s,k}^{(FEC)}$. As a result, the PGF $T_{ov}(z)$ of the service time distribution for j

aggregated MPDUs can be obtained as

$$T_{ov}(z) = \sum_{j=\alpha}^{\beta} p_j \cdot [T(z)]^j \quad (4.27)$$

where p_j is acquired from (4.12).

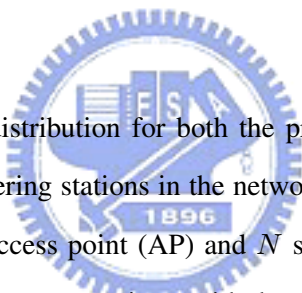
4.3 Iteration Algorithm for Proposed ARQ Schemes

In order to calculate the service time distributions (i.e. (4.16) and (4.27)) for both the proposed ASR-ARQ and AH-ARQ schemes, an iteration algorithm is required to be exploited. The procedures of the iterative algorithm is listed as follows:

1. The algorithm starts with the saturation case with $[p_{\alpha} \dots p_{\beta}] = [00 \dots 01]$ and $[\pi_0 \dots \pi_K] = [00 \dots 01]$.
2. Calculate the PDFs of the MAC service time for either the ASR-ARQ scheme (i.e. (4.16)) or the AH-ASR scheme (i.e. (4.27)).
3. Compute the transition probability $k_j \simeq \sum_{i=0}^{\infty} t_i e^{-\lambda i} \frac{(\lambda i)^j}{j!}$. It is noted that $1 \mu s$ is taken as the time unit and t_i denotes the probability that the service time is $i \mu s$. Consequently, the newly updated $[\pi_0 \dots \pi_K]$ could be calculated.
4. The PDF of the MAC service time is recalculated via either (4.16) or (4.27). Compare the PDF with the previous computed value from step 2. If the value converges, the process stops here. Otherwise, the process goes to step 3.

Chapter 5

Performance Analysis of Proposed ARQ Schemes with Existence of Interfering Stations



In this chapter, the service time distribution for both the proposed ARQ schemes are acquired by considering the existence of interfering stations in the network. The centralized network topology is considered, where there are one access point (AP) and N stations. The N stations are contending for accessing the channel in order to communicate with the AP for data transmission. For simplicity, saturated queuing model is considered in this section, i.e. each station consistently has frames to be delivered. Section 5.1 described the modeling of service time distribution for the proposed ASR-ARQ scheme; while that of the AH-ARQ algorithm is presented in Section 5.2, where the existence of collision probability is considered in both cases.

5.1 Modeling of Service Time Distribution of Proposed ASR-ARQ Scheme with Contending Stations

In this section, the service time distribution for the ASR-ARQ scheme in the existence of contending stations is derived. Three components are required to be obtained for the derivation of the service

time distribution $T_{total}(z)$, i.e. the conditional PGF of consecutive back-off time slot $H_d(z)$, the conditional PGF $E_{m,f}(z)$ caused by failed retransmissions, the and conditional PGF $S_n(z)$ of successful transmission time. First of all, the conditional PGF of consecutive back-off time slot $H_d(z)$ is derived via Mason's gain rule [25] as

$$H_d(z) = \frac{(1-p_c)z^\sigma}{1-(p_c-p_s)C(z)-p_sM(z)}. \quad (5.1)$$

where $(p_c-p_s)C(z)+p_sM(z)$ and $(1-p_c)z^\sigma$ corresponds to the loop gain and the open loop gain respectively. The collision probability p_c and the successful transmission probability p_s can be obtained as from (3.8) and (3.9) via the Markov chain model. It is noted that $C(z) = z^{T_{RTS}+T_{SIFS}+T_{CTS}+T_{DIFS}}$, and the conditional PGF $M(z)$ of transmission time interrupted via another station is acquired as

$$M(z) = \sum_{m=0}^{R-1} \frac{b_{m,0}}{\tau(1-p_{m,0}^j)} \sum_{k=1}^j p_{m,k}^j \{ (1-p_{f,e})^k z^{T_{RTS}+T_{CTS}+3T_{SIFS}+k\eta+T_{BA}+T_{DIFS}+} \\ \sum_{l=1}^k \sum_{n=0}^l C_l^k C_n^l p_{f,e}^{l+n} (1-p_{f,e})^{k-n} z^{T_{RTS}+T_{CTS}+5T_{SIFS}+2T_{BA}+(k+l)\eta+T_{DIFS}} \} \quad (5.2)$$

where the probability $p_{m,k}^j$ in (5.2) is acquired as $p_{m,k}^j = [\mathbf{v}_{1 \times (j+1)}^{(m)}]_{k+1}$. The vector $\mathbf{v}_{1 \times (j+1)}^{(m)}$ is obtained via $\mathbf{v}_{1 \times (j+1)}^{(m)} = \mathbf{v}_{1 \times (j+1)}^{(0)} \times \mathbf{T}^m$ with initial probability vector $\mathbf{v}_{1 \times (j+1)}^{(0)} = [0 \ 0 \ \dots \ 0 \ 1]$. The elements within the transition matrix $\mathbf{T}_{(j+1) \times (j+1)}$ is obtained as

$$p_{i,j} = \begin{cases} 1, & i = j = 0 \\ p_c + (1-p_c)p_{f,e}^{2i}, & 1 \leq i \leq j, j = i \\ (1-p_c) \sum_{k=0}^{i-j} C_k^i C_{i-j-k}^{i-k} (1-p_{f,e})^{i-j} p_{f,e}^{i+j-k}, & 0 \leq j < i \\ 0, & j > i \end{cases} \quad (5.3)$$

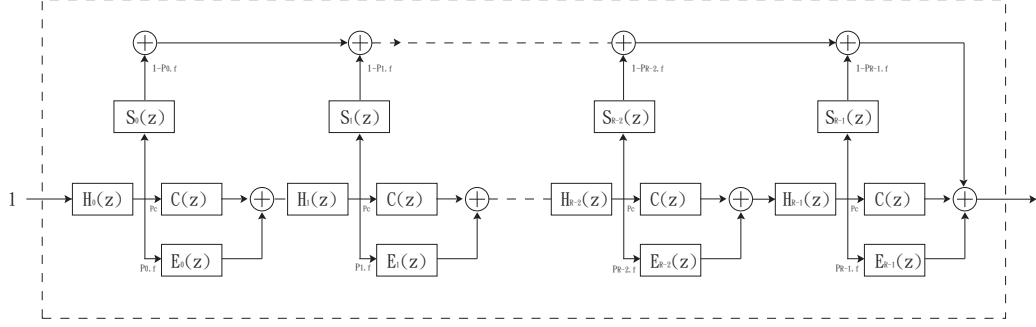


Figure 5.1: Service System Diagram.

Moreover, the conditional PGF $E_{m,f}(z)$ resulted from the error retransmissions between the m th and the $(m + 1)$ th back-off stages is computed as

$$E_{m,f}(z) = \sum_{k=1}^j \frac{p_{m,k}^j}{(1 - p_{m,0}^j) p_{s,k}} \sum_{i=1}^k \sum_{l=1}^i C_i^k C_l^i p_{f,e}^{l+i} (1 - p_{f,e})^{k-l} z^{T_{RTS} + T_{CTS} + 5T_{SIFS} + 2T_{BA} + (k+i)\eta + T_{DIFS}} \quad (5.4)$$

where $p_{s,k} = 1 - \sum_{v=0}^k C_v^k p_{f,e}^v (1 - p_{f,e})^k$. The defined probability $p_{m,0}^j$ can be also acquired as

$$p_{m,0}^j = \sum_{k=1}^m \frac{d^k F_j(D)}{k! d D^k} \quad (5.5)$$

where

$$F_j(D) = \sum_{k=0}^j \frac{j!}{(j-k)! k!} \frac{(-1)^k (1-D)}{1 - p_c D - (1-p_c) D p_{f,e}^{2k}} \quad (5.6)$$

It is noticed that the recurrent function $F_j(D)$ in this case is considered for the mechanism of selective-repeat retransmission, where the collision probability p_c is included. Furthermore, the conditional PGF $S_n(z)$ for the successful transmission time between the n th and the $(n + 1)$ th stages is

depicted as

$$S_n(z) = \sum_{k=1}^j \frac{p_{n,k}^j}{(1-p_{n,0})p_{\epsilon,k}} \{(1-p_{f,e})^k z^{T_{RTS}+T_{CTS}+3T_{SIFS}+k\eta+T_{BA}+T_{DIFS}+} + \sum_{i=1}^k C_i^k p_{f,e}^i (1-p_{f,e})^k z^{T_{RTS}+T_{CTS}+5T_{SIFS}+2T_{BA}+T_{DIFS}+(k+i)\eta}\} \quad (5.7)$$

where $p_{\epsilon,k} = 1 - \sum_{i=1}^k \sum_{l=1}^i C_i^k C_l^i p_{f,e}^{l+i} (1-p_{f,e})^{k-l}$. As a result, the PGF of total service time distribution $T_{total}(z)$ referred as Fig. (5.1) is obtained as

$$T_{total}(z) = (1-p_{0,f})H_0(z)S_0(z) + \sum_{i=1}^{R-1} \left[\prod_{k=0}^i H_k(z) \right] \left[\prod_{l=0}^{i-1} (p_c C(z) + (p_{l,f} - p_c)E_{l,f}(z)) \right] \\ (1-p_{i,f})S_i(z) + \prod_{i=0}^{R-1} H_i(z) \prod_{m=0}^{R-1} (p_c C(z) + (p_{m,f} - p_c)E_{m,f}(z)) \quad (5.8)$$

where the failed transmission probability $p_{m,f}$ at the m th stage is acquired as

$$p_{m,f} = p_c + (1-p_c) \sum_{k=1}^j p_{m,k}^j p_{s,k}. \quad (5.9)$$

5.2 Modeling of Service Time Distribution of Proposed AH-ARQ Scheme with Contending Stations

In this subsection, the service time distribution for the proposed AH-ARQ scheme with the consideration of channel contention is addressed.

With the collision probability considered for the aggregated MPDUs, the PMF of the random variable X that represents the number of retransmissions until all MPDUs have been positively acknowledged is denoted as

$$P_X(x) = \sum_{k=0}^x C_k^x p_c^k (1-p_c)^{x-k} \left[\left(\sum_{i=1}^{x-k} \frac{d^i F_N(D)}{i! dD^i} \right)^j u(x-k) - \left(\sum_{i=1}^{x-k-1} \frac{d^i F_N(D)}{i! dD^i} \right)^j u(x-k-1) \right] \quad (5.10)$$

where $u(x) = 1$ if $x > 0$ and $u(x) = 0$ for $x \leq 0$. It is noticed that recursion function $F_N(D)$ can be obtained from (4.19), which addresses the retransmission mechanism on the RS-block basis. Similarly, the conditional PGF $E_{m,f}(z)$ for unsuccessful transmissions between the m th and the $(m+1)$ th stages is modified for addressing the AH-ARQ scheme as

$$E_{m,f}(z) = \sum_{v=0}^m C_v^m \frac{p_c^v (1-p_c)^{m-v}}{1 - (p_{m-v,0}^N)^j} \sum_{x=0}^{j-1} C_x^j \frac{(p_{m-v,0}^N)^x (1 - p_{m-v,0}^N)^{j-x}}{1 - [\sum_{k=1}^N \frac{p_{m-v,k}^N}{1-p_{m-v,0}^N} (1 - p_{s,k}^{(FEC)})]^{j-x}} \sum_{i=0}^{j-x-1} C_i^{j-x} [A(m, v, z)^i B(m, v, z)^{j-x-i} \cdot z^{T_{RTS} + T_{CTS} + 5T_{SIFS} + 2T_{BA} + T_{DIFS}}] \quad (5.11)$$

where

$$A(m, v, z) = \sum_{k=1}^N \frac{p_{m-v,k}^N}{1 - p_{m-v,k}^N} [(1 - P_e)(1 - P_{block,e})^k z^{t_{oh} + k\eta} + P_e(1 - P_e)(1 - P_{block,e})^k z^{2t_{oh} + 2k\eta} + (1 - P_e)^2 \sum_{l=1}^k C_l^k P_{block,e}^l (1 - P_{block,e})^k z^{2t_{oh} + (k+l)\eta}] \quad (5.12)$$

$$B(m, v, z) = \sum_{k=1}^N \frac{p_{m-v,k}^N}{1 - p_{m-v,0}^N} [P_e^2 z^{2t_{oh} + 2k\eta} + (1 - P_e)P_e \sum_{i=1}^k C_i^k P_{block,e}^i (1 - P_{block,e})^{k-i} z^{2t_{oh} + (k+i)\eta} + (1 - P_e)P_e \sum_{i=1}^k C_i^k P_{block,e}^i (1 - P_{block,e})^{k-i} z^{2t_{oh} + 2k\eta} + (1 - P_e)^2 \sum_{i=1}^k \sum_{l=1}^i C_i^k C_l^i (1 - P_{block,e})^{k-l} P_{block,e}^{i+l} z^{2t_{oh} + (k+i)\eta}]. \quad (5.13)$$

Note that $p_{m-v,k}^N$, $k > 0$ is defined in section 5.2, and from

$$\sum_{k=0}^x C_k^x p_c^k (1-p_c)^{x-k} [(p_{x-k,0}^N)^j u(x-k) - (p_{x-k-1,0}^N)^j u(x-k-1)] = P_X(x), \quad (5.14)$$

$p_{m-v,0}^N$ could also be derived. It is noted that the $1 - (p_{m-v,0}^N)^j$ within (5.11) represents the normalized term, which corresponds to the probability that not all MPDUs have been successfully transmitted before the m th stage. The normalization probability $1 - [\sum_{k=1}^N \frac{p_{m-v,k}^N}{1-p_{m-v,0}^N} (1 - p_{s,k}^{(FEC)})]^{j-x}$ represents the probability which excludes the case that all $(j-x)$ MPDUs have been successfully delivered at the m th stage. It is noted that $p_{s,k}^{(FEC)}$ is obtainable from chapter 5. Moreover, the conditional PGF

$S_m(z)$ for the successful transmission time between the m th and $(m + 1)$ th stages is acquired as

$$S_m(z) = \sum_{v=0}^m C_v^m \frac{p_c^v (1-p_c)^{m-v}}{1-(p_{m-v,0}^N)^j} \sum_{x=1}^j C_x^j \frac{(1-p_{m-v,0}^N)^x (p_{m-v,0}^N)^{j-x}}{[\sum_{k=1}^N \frac{p_{m-v,k}^N}{1-p_{m-v,0}^N} p_{\epsilon,k}^{(FEC)}]^x} [z^{T_{RTS}+3T_{SIFS}+T_{CTS}+T_{BA}+T_{DIFS}} \tilde{B}(m, v, z)^x + z^{T_{RTS}+T_{CTS}+5T_{SIFS}+2T_{BA}+T_{DIFS}} \sum_{i=1}^x C_i^x \tilde{A}(m, v, z)^i \tilde{B}(m, v, z)^{x-i}] \quad (5.15)$$

where

$$\tilde{A}(m, v, z) = \sum_{k=1}^N \frac{p_{m-v,k}^N}{1-p_{m-v,0}^N} [P_e(1-P_e)(1-P_{block,e})^k z^{2t_{oh}+2k\eta} + (1-P_e)^2 \sum_{l=1}^k C_l^k P_{block,e}^l (1-P_{block,e})^k z^{2t_{oh}+(k+l)\eta}] \quad (5.16)$$

$$\tilde{B}(m, v, z) = \sum_{k=1}^N \frac{p_{m-v,k}^N}{1-p_{m-v,0}^N} [(1-P_e)(1-P_{block,e})^k z^{t_{oh}+k\eta}] \quad (5.17)$$

It is noted that that the normalization term $[\sum_{k=1}^N \frac{p_{m-v,k}^N}{1-p_{m-v,0}^N} p_{\epsilon,k}^{(FEC)}]^x$ denotes the probability that all the remaining MPDUs have been successfully retransmitted at the m th stage. $\tilde{A}(m, v, z)$ and $\tilde{B}(m, v, z)$ represent the transfer function of transmitting time that take one or two transmission opportunities respectively. Furthermore, the conditional PGF of consecutive backoff time slot $H_d(z)$ can be obtained from (5.1), where the conditional PGF $S(z)$ for of transmission time that is interrupted by another station is acquired as

$$M(z) = \sum_{i=0}^{R-1} \frac{b_{i,0}}{\tau} \sum_{x=0}^i C_x^i \frac{p_c^x (1-p_c)^{i-x}}{1-(p_{i-x,0}^N)^j} \sum_{v=1}^j C_v^j (1-p_{i-x,0}^N)^v (p_{i-x,0}^N)^{j-v} [z^{T_{RTS}+T_{CTS}+3T_{SIFS}+T_{BA}} \tilde{B}(i, x, z)^v + z^{T_{RTS}+T_{CTS}+5T_{SIFS}+2T_{BA}+T_{DIFS}} \sum_{l=1}^v C_l^v \tilde{A}(i, x, z)^l \tilde{B}(i, x, z)^{v-l} + z^{T_{RTS}+T_{CTS}+5T_{SIFS}+2T_{BA}+T_{DIFS}} \sum_{r=1}^v C_r^v B(i, x, z)^r A(i, x, z)^{v-r}] \quad (5.18)$$

As a result, the PGF of total service time distribution $T_{total}(z)$ is obtained as

$$T_{total}(z) = (1 - p_{0,f})H_0(z)S_0(z) + \sum_{i=1}^{R-1} \left[\prod_{k=0}^i H_k(z) \right] \left[\prod_{l=0}^{i-1} (p_c C(z) + (p_{l,f} - p_c)E_{l,f}(z)) \right] \\ (1 - p_{i,f})S_i(z) + \prod_{i=0}^{R-1} H_i(z) \prod_{m=0}^{R-1} (p_c C(z) + (p_{m,f} - p_c)E_{m,f}(z)) \quad (5.19)$$

where

$$p_{m,f} = p_c + (1 - p_c) \sum_{v=0}^m C_v^m p_c^v (1 - p_c)^{m-v} \sum_{i=1}^j C_i^j (1 - p_{m-v,0}^N)^i (p_{m-v,0}^N)^{j-i} \\ \sum_{l=1}^i C_i^l \left[\sum_{k=1}^N \frac{p_{m-v,k}^N}{1 - p_{m-v,0}^N} p_{s,k}^{(FEC)} \right]^l \left[\sum_{k=1}^N \frac{p_{m-v,k}^N}{1 - p_{m-v,0}^N} p_{\epsilon,k}^{(FEC)} \right]^{i-l} \quad (5.20)$$

It is noted that the failed transmission probability $E_{m,f}(z)$ at the m th stage is obtained from (5.7).¹



¹The above equation (5.11) - (5.20) might suffer the case 0^0 when $m = v$, $k = 0$, $p_{m-v,k}^N = 0$. Here we treated the 0^0 equaling one.

Chapter 6

Performance Evaluation

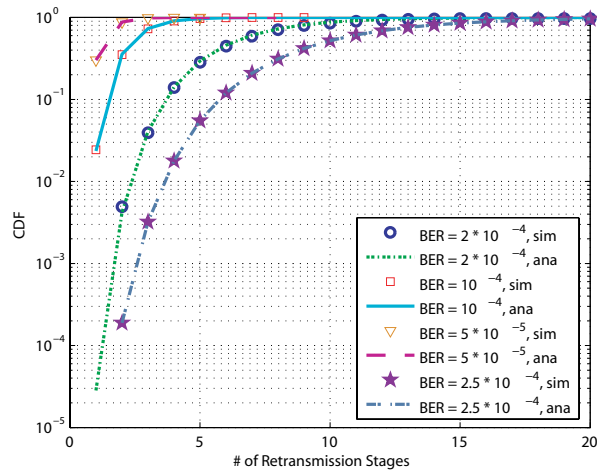
In this section, the numerical and simulation results are computed and verified for error prone channels. The systemC/C++ simulation models are constructed based on the parameters listed in Table 6. It was considered a one hop network in the following discussions. The channel considered following regards PHY as a binary symmetric channel (BSC) and we omit the effects of PCLP protocols (i.e. synchronization errors, Tx period). First, we validate the analysis model of required retransmissions of both retransmission mechanisms under different BERs or aggregation numbers with existing of only one reverse/forward link. Fig. (6.1(a)) shows the distribution that the number of required retransmission times until all aggregated MPDUs have been positive acknowledged through the conventional ASR-ARQ. The number of aggregated MPDUs is fixed 10 with each MPDU size configured 1024 bytes and it has been validated at four different BERs. It could be observed that as the increment of number of retransmissions, the improvement of frame error rate becomes bigger at higher BERs. Fig. (6.1(b)) shows the cumulated density function of necessary retransmissions through AH-ARQ scheme instead. The (255,223,16) RS code for AH-ARQ over $GF(2^8)$ constructed via the primitive polynomial $1 + x^2 + x^3 + x^4 + x^8$ is defined. Each 835-byte-long packet within A-MPDU consists of three RS blocks which excludes the header and delimiter blocks. The differences among simulation and analysis results could be explained from the upper bounded decoding error probability $P_{block,e}$ as defined in equation 4.17. We have concluded while it is with more aggregated packets, the advantages of boosting the retried times is more significant. Following we show the MAC service time

distributions which are modeled in the previous sections. It further be confirmed with more than one STA concurrently access the channel (i.e. NoS = 3) under two different BERs. First, an unsaturation scenario with NoS = 1 is validated. The packets aggregated varies within [5, 10] according to the minimum batch rule and the arrival rate λ is set 100 fps, queue length $K = 20$. The iteration algorithm described in previous section is applied for analysis purpose. We have found that the iteration algorithm could be converged within 5 iterative steps (i.e. iteration converges at 3rd step for ASQ-ARQ and 4th step for AH-ARQ respectively). The slightly differences among simulation and analytical results could be explained from the assumption of Markov ergotic process within queuing models and the approximated formulas for decoding error probability. For NoS = 3, the saturation scenario is considered based on previous assumptions from Fig. (6.6) to Fig. (6.9). The number of packets aggregated is fixed and varies from 5 to 20 varies with two different BERs for comparison purpose. The differences among analytical and simulation results could be explained that the sampling time for Markov chain model is based on a time slot(i.e. σ) instead of variable time period. However, it could be observed that our analytical models give well estimation of MAC service time distribution. Fig. (6.2) to Fig. (6.3) show the results of the normalized saturation MAC layer throughput and average MAC service delay with number of contenting STAs equals 6 and 18 respectively (i.e. NoS = 6, NoS = 18). While the throughput is defined as the average bytes of information payload successfully received by receiver divided by the average time required to deliver them while accounting to the retried limit. An aggregated MSDUs mechanism is also implemented for comparison purpose. In the aggregated MSDUs scheme(AMS), a MPDU consists of multiple MSDUs, that means the MSDUs share common FCS and MAC header. The aggregated size of information payloads for each mechanism is set equal for fairly comparisons. We observe that AH-ARQ outperforms the rest two mechanisms under high BERs. For lower BERs, the overhead introduced by parity symbols within AH-ARQ resulted in poorer throughput. However, the considerable throughput gain is obtained across a broad range of BERs. The two AMS and ASR-ARQ suffer similar saturated throughput under low BERs, for the sake that failed retransmissions are mainly caused via collision effects. It could be also observed that the average access delay of AMS scheme is shorter than the ASR scheme under high BERs. It could be explained that for high BERs, since almost all packets are retransmitted in each transmission oppor-

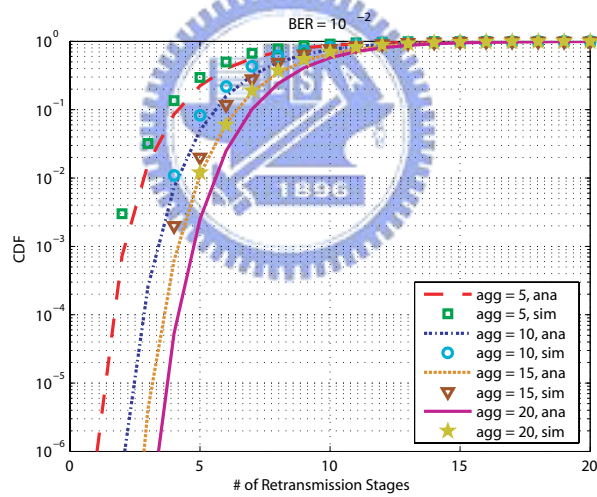
MAC Defined Parameters	
RTS	20 bytes
CTS	14 bytes
BACK	32 bytes
MAC_HDR	28 bytes
DIFS	34 μs
SIFS	16 μs
σ	9 μs
Retry_Limit	7
CW_{min}	8
CW_{max}	512
Data Rate	24 Mbps

Table 6.1: Simulation Parameters.

tunity, the redundancy introduced through delimiters and MAC headers for ASR is more than ASM scheme. For NoS = 18, since the access time is increased owing to longer contention period and more collision opportunities, the throughput is then decreased comparing to NoS = 6. It could be further observed that there is no definite superiority of increasing number of aggregated MPDUs, especially the ASR-ARQ and AMS schemes. It could be explained from the trade-off between access delay and effective transmitted information payloads. For more aggregated MPDUs, it makes the transmission time much longer and postpones the back-off delay. For AH-ARQ mechanism, since the FEC reduces the retransmission possibility, the longer delay impacts are not obvious. However, the increment of successfully transmitted information payloads is finite. Therefore, we have to aware whether the channel is good enough (low BERs) especially while applying ASR-ARQ in order to have positive gain on the promotion of throughput with frame aggregation mechanism.

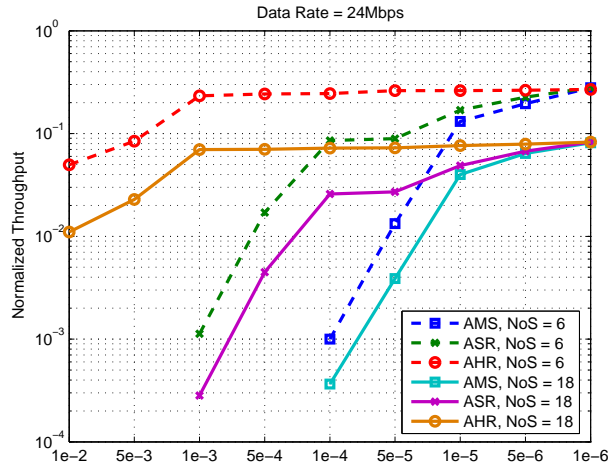


(a)

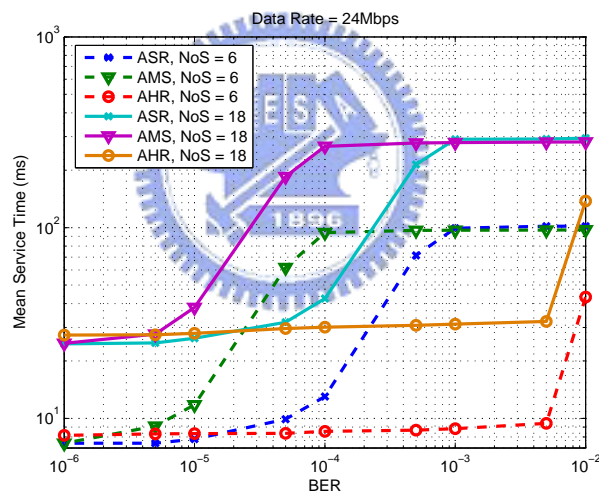


(b)

Figure 6.1: (a) Cumulated Density Function versus Number of Retransmission Stages with ASR mechanism. The A-MPDU consists of 10 MPDUs. (b) Cumulated Density Function versus Number of Retransmission Stages with AHR mechanism. Each MPDU consists of 3 RS Blocks.

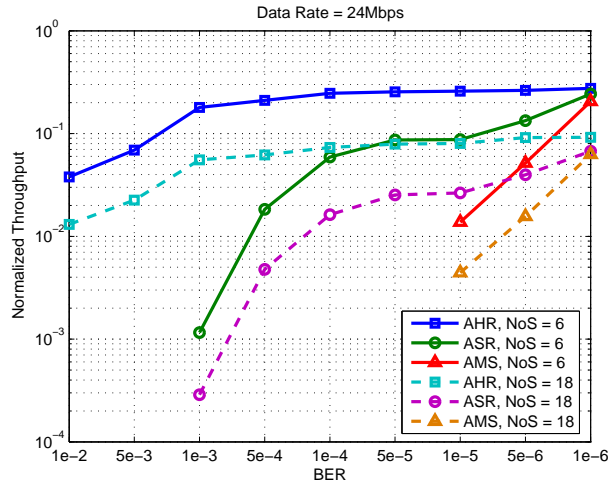


(a)

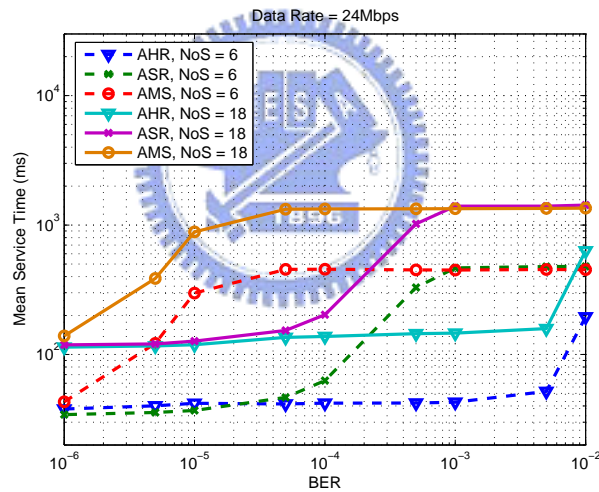


(b)

Figure 6.2: An aggregated frame consists of 10 MPDUs for AH-ARQ (AHR) and ASR-ARQ (ASR). For pure aggregated MSDU mechanism (AMS), there are same number(10) of MSDUs within a MPDU. The information payload is 657- byte-long within a MPDU in ASR and ASR schemes. For AMS, the MSDU consists of 657 bytes information payload. (a) Normalized MAC Throughput, (b) Mean Service Time.



(a)



(b)

Figure 6.3: An aggregated frame consists of 50 MPDUs for AH-ARQ (AHR) and ASR-ARQ (ASR). For pure aggregated MSDU mechanism (AMS), there are same number(50) of MSDUs within a MPDU. The information payload is 657- byte-long within a MPDU in ASR and ASR schemes. For AMS, the MSDU consists of 657 bytes information payload. (a) Normalized MAC Throughput, (b) Mean Service Time.

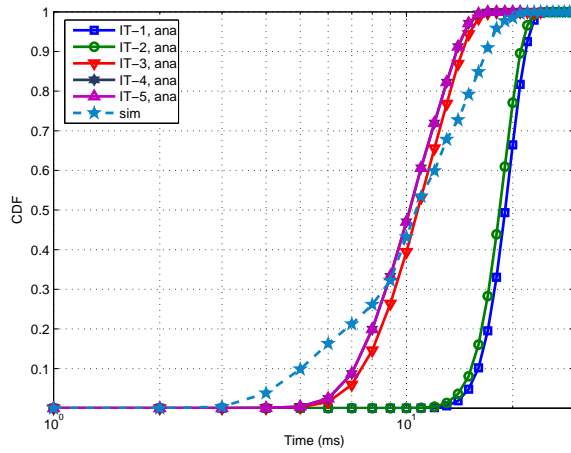


Figure 6.4: MAC Service Time Distribution of AH-ARQ under $BER = 10^{-2}$, $[\alpha, \beta] = [5, 10]$, unsaturation case with five iterations. Number of RS blocks = 3, and each RS block consists of 219-byte-long information octets.

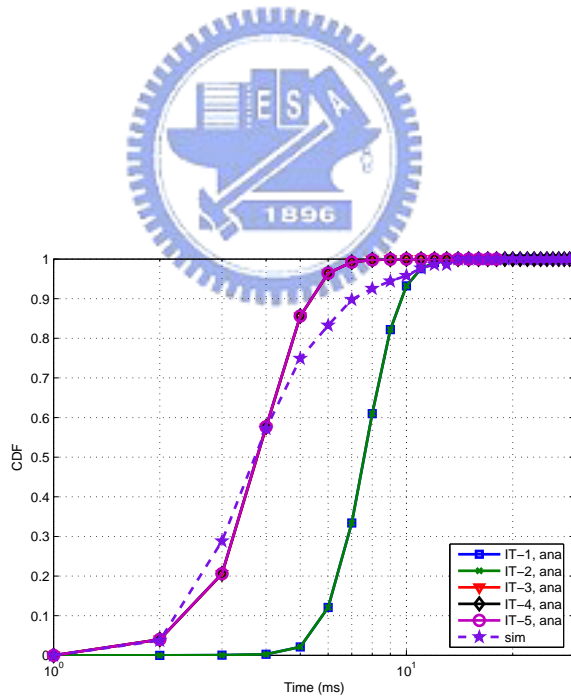


Figure 6.5: MAC Service Time Distribution of ASR-ARQ under $BER = 2 \times 10^{-4}$, $[\alpha, \beta] = [5, 10]$, unsaturation case with five iterations. Each MPDU consists of 657-byte-long information payload.

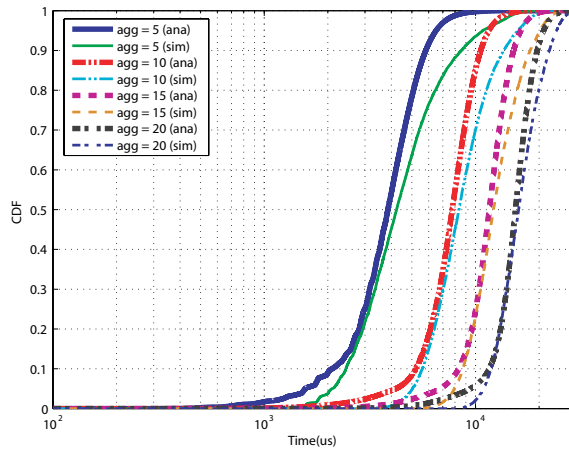


Figure 6.6: Cumulated Density Function of ASR-ARQ Scheme under $BER = 2 \times 10^{-4}$, saturation case. NoS = 3, and each MPDU consists of 657-byte-long information payload.

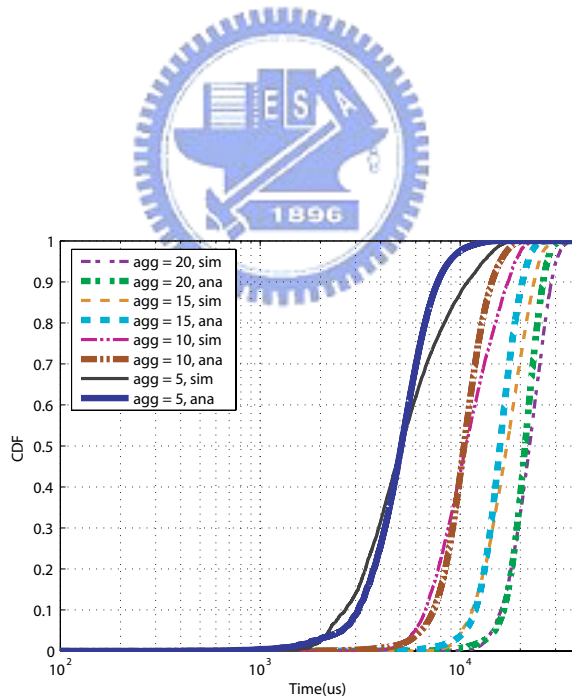


Figure 6.7: Cumulated Density Function of ASR-ARQ Scheme under $BER = 2.5 \times 10^{-4}$, saturation case. NoS = 3, and each MPDU consists of 657-byte-long information payload.

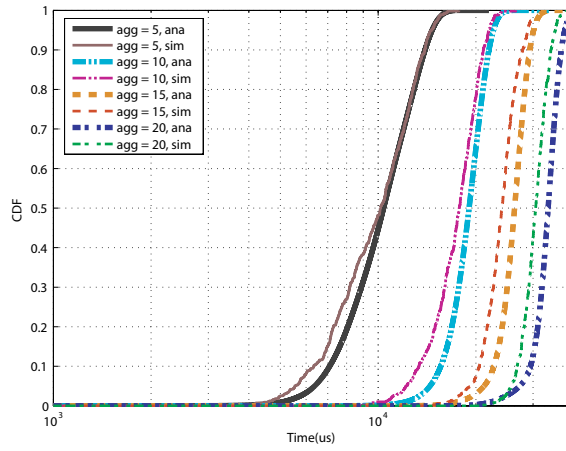


Figure 6.8: Cumulated Density Function of AHR-ARQ Scheme under $BER = 10^{-2}$, saturation case. NoS = 3, number of RS blocks = 3, and each RS block consists of 219-byte-long information octets.

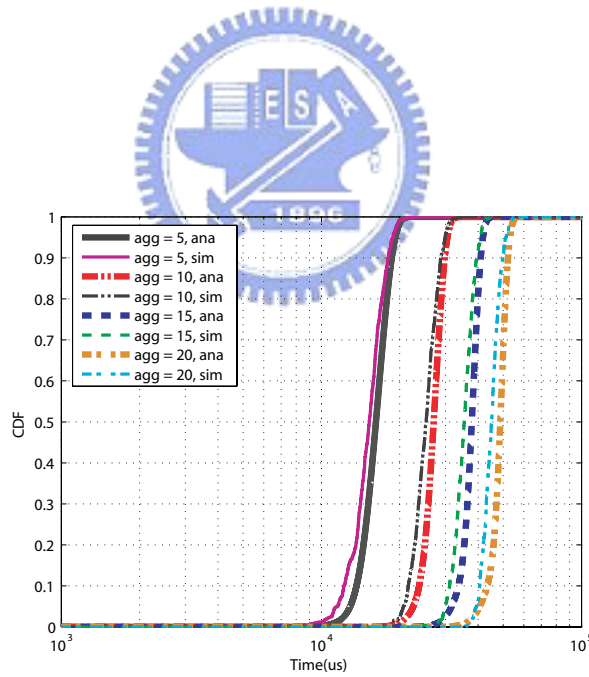
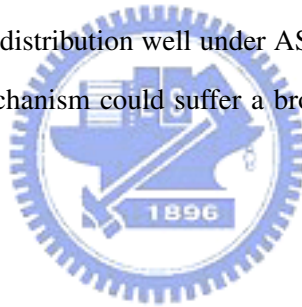


Figure 6.9: Cumulated Density Function of AHR-ARQ Scheme under $BER = 1.1 \times 10^{-2}$, saturation case. NoS = 3, number of RS blocks = 3, and each RS block consists of 219-byte-long information octets.

Chapter 7

Conclusion

In this paper, we develop an analytical model to evaluate the performance of AH-ARQ or ASR-ARQ applied on IEEE 802.11n in binary symmetric channels, in which MPDUs might fail due to bit transition errors. Extensive simulation and numerical results show that the analytical model proposed can predict the MAC service time distribution well under ASR-ARQ or AH-ARQ schemes. Furthermore, the proposed AH-ARQ mechanism could suffer a broad range of BERs but still has positive throughput gain.

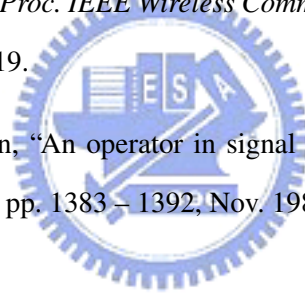


Bibliography

- [1] “Tgn sync proposal technical specification,” *IEEE 802.11n TGN Sync*.
- [2] “Wwise proposal : High throughput extension to the 802.11 standard,” *IEEE 802.11n WWiSE*.
- [3] “Ht mac specification,” *Enhanced Wireless Consortium*.
- [4] Y. Li, S. W. Kim, J. K. Chung, and H. G. Ryu, “Sfbc-based mimo ofdm and mimo ci-ofdm systems in the nonlinear and nbi channel,” in *Proc. IEEE Communications, Circuits and Systems*, vol. 2, June 2006, pp. 898–901.
- [5] Y. Li, X. Wang, and S. A. Mujtaba, “Impact of physical layer parameters on the mac throughput of ieee 802.11 wireless lans,” in *Proc. IEEE Signals, Systems and Computers Conference*, vol. 2, Nov. 2004, pp. 1468–1472.
- [6] D. Skordoulis, N. Qiang, H. H. Chen, A. P. Stephens, C. Liu, and A. Jamalipour, “Ieee 802.11n mac frame aggregation mechanisms for next-generation high-throughput wlans [medium access control protocols for wireless lans],” *IEEE Trans. Wireless Commun.*, vol. 15, pp. 40–47, Feb. 2008.
- [7] D. L. Lu and J. F. Chang, “Analysis of arq protocols via signal flow graphs,” *IEEE Trans. Commun.*, vol. 37, pp. 245 – 251, Mar. 1989.
- [8] Y. Hua and Z. Niu, “An analytical model for ieee 802.11 wlans with nak-based arq mechanism,” in *Proc. APCC on Communications*, 2007.

- [9] J. B. Seo, N. H. Park, H. W. Lee, and C. H. Cho, "Impact of an arq scheme in the mac/llc layer on upper-layer packet transmissions over a markovian channel," in *Proc. IEEE 63rd Vehicular Technology Conference*, vol. 4, 2006.
- [10] K. C. Beh, A. Doufexi, and S. Armour, "Performance evaluation of hybrid ARQ schemes of 3gpp lte ofdma system," in *Proc. IEEE 18th Personal, Indoor and Mobile Radio Communications*, 2007.
- [11] E. Malkamaki, D. Mathew, and S. Hamalainen, "Performance of hybrid ARQ techniques for WCDMA high data rates," in *Proc. IEEE 53rd Vehicular Technology Conference*, vol. 4, May 2001, pp. 2720–2724.
- [12] T. F. Wong, L. Gao, and T. M. Lok, "A type-i hybrid ARQ protocol over optimal-sequence CDMA link," in *Proc. IEEE 21st Century Military Communications*, vol. 1, Oct. 2001, pp. 559–563.
- [13] J. F. Cheng, Y. P. E. Wang, and S. Parkvall, "Adaptive incremental redundancy [wcdma systems]," in *Proc. IEEE 58th Vehicular Technology Conference*, vol. 2, 2003.
- [14] Q. Chen and P. Fan, "On the performance of type-iii hybrid arq with rcp codes," in *Proc. IEEE Personal, Indoor and Mobile Radio Communications*, vol. 2, Sept. 2003, pp. 1297–1301.
- [15] R. Guo and J. L. Liu, "Ber performance analysis of rcp encoded MIMO-OFDM in nakagami-m channels," in *Proc. IEEE Information Acquisition Conference*, 2006.
- [16] Proakis, "*Digital Communications 4th Edition*", McGRAW-HILL, 2001.
- [17] U. Cheng, "On the continued fraction and berlekamp's algorithm," *IEEE Trans. Inform. Theory*, vol. 30, pp. 541 – 544, May 1984.
- [18] M. A. Khan, S. Afzal, and R. Manzoor, "Hardware implementation of shortened (48,38) reed solomon forward error correcting code," in *Proc. INMIC Multi Topic Conference*, 2003.
- [19] G. Bianchi, "Performance analysis of the ieee 802.11 distributed coordination function," *IEEE J. Select. Areas Commun.*, vol. 18, pp. 535 – 547, Mar. 2000.

- [20] O. Tickoo and B. Sikdar, "Queueing analysis and delay mitigation in ieee 802.11 random access mac based wireless networks," in *Proc. IEEE INFOCOM*, vol. 2, Mar. 2004, pp. 1404 – 1413.
- [21] Y. Zheng, K. Lu, D. Wu, and Y. Fang, "Performance analysis of ieee 802.11 dcf in binary symmetric channels," in *Proc. IEEE Global Telecommunications Conference*, vol. 5, Nov. 2005, pp. 3144–3148.
- [22] Y. Lin and V. W. S. Wong, "Frame aggregation and optimal frame size adaptation for ieee 802.11n wlans," in *Proc. IEEE Global Telecommunications Conference*, 2006.
- [23] S. Kuppa and G. R. Dattatreya, "Modeling and analysis of frame aggregation in unsaturated wlans with finite buffer stations," in *Proc. IEEE International Conference on Communications*, 2006.
- [24] C. W. Liu and A. P. Stephens, "An analytic model for infrastructure wlan capacity with bidirectional frame aggregation," in *Proc. IEEE Wireless Communications and Networking Conference*, vol. 1, Mar. 2005, pp. 113–119.
- [25] M. Sengoku and W. K. Chen, "An operator in signal flow graphs and its applications," *IEEE Trans. Circuits Syst.*, vol. 35, pp. 1383 – 1392, Nov. 1988.



Part II

Efficient Implementation of an Energy-Conserving Multicast Routing Protocol for Wireless Multihop Networks



Chapter 8

Introduction

With the emergent applications for multicast data dissemination and aggregation, the design of multicast routing algorithms are considered one of the important topics within the Wireless Multihop Networks (WMNs). Basically, these protocols can be categorized into the tree-based (such as MAODV [1], AMRIS [2], AMRoute [3], and GS [4]) and the mesh-based (such as ODMRP [5] [6], CAMP [7], and MCEDAR [8]) algorithms. The fundamental topology of the tree-based network originates from a root, which stretches out its branches and the corresponding sub-branches. The benefit of using the tree-based structure can be attributed to its low energy consumption and the simplicity for maintaining the structure in static networks. In the mesh-based structure, there are at least two routes between each receiver and transmitter. Comparing with the tree-based networks, this architecture can provide more robust connectivity under the channel fading effect. However, the inherent complexity within the mesh-based structure makes it consume more system resources.

Most of the existing multicast routing protocols within the WMNs are considered not feasible for practical implementation either due to the protocol complexity or the excessive rerouting expenses. In this paper, an Energy-Conserving Multicast Routing (ECMR) protocol is proposed for reducing the number of data transmissions within the WMNs. Since obtaining the minimum cost multicast tree under the wireless broadcast environment is proved to be an NP-Hard problem [9], a heuristic algorithm is exploited by the ECMR scheme for energy conservation purpose. By adopting the proposed algorithm, the conventional multicast structure (e.g. the ODMRP protocol [6]) can be converged into

a light-weight topology. The total energy consumption can therefore be decreased; while the packet delivery ratio is still maintained. Field experiments are conducted in order to evaluate the performance of the proposed algorithm. Based on the experiment results, the ECMR protocol is capable of providing better energy conservation comparing with the existing ODMRP algorithm.

The remainder of this part is organized as follows. The proposed ECMR protocol is presented in chapter 9. chapter 10 describes the implementation architecture and the experimental results for the evaluation of the proposed ECMR protocol. chapter 11 draws the conclusions.



Chapter 9

The Proposed Energy-Conserving Multicast Routing (ECMR) Protocol

9.1 The Concept of Heuristic Structure Construction

In order to provide bandwidth efficiency, the proposed ECMR protocol establishes the multicast routes via the source-initiated and on-demand manners. The structure constructed by the ECMR algorithm can be represented as $\mathcal{T} = \{S, \mathbf{I}, \mathbf{R}\}$, where S denotes the source node, $\mathbf{I} = \{I_i | \forall i \in \mathbb{N}\}$ and $\mathbf{R} = \{R_i | \forall i \in \mathbb{N}\}$ represent the sets of intermediate nodes and receiving nodes. There are two important parameters introduced within the ECMR protocol, which are denoted as the N_WGHT field within each node and the P_WGHT field for each constructed path. Both the N_WGHT and the P_WGHT parameters are utilized to indicate the significance of its corresponding node and route within the constructed structure \mathcal{T} .

The route request/reply process utilized in most of the on-demand unicast routing protocols is modified and employed within the proposed ECMR algorithm. The source node S advertises the join request (JREQ) packets for both initiating and updating the multicast routes within the structure \mathcal{T} . It is noted that the structure updates are conducted periodically with the time interval set by the JREQ Flood Timeout (FLDT) parameter. Initially, S will flood the JREQ packets (which include the ID of S) to its neighbor nodes while it has packets to be transmitted to the receiver set \mathbf{R} . After the intermediate

node I_i receives the first JREQ packet, it will wait for the Collection Time of the Intermediate node (CT_I) in order to obtain the other JREQ packets, which can be routed from other paths to I_i . After the collection time has expired, I_i will select the JREQ packet with its corresponding path that has the largest weight, i.e. the path $P_i = \max_{v_k} \{P_k.P_WGHT\}$. It is noted that the value recorded within the $P_i.P_WGHT$ parameter is accumulated by the N_WGHT values of the nodes that consist of the corresponding path P_i . The intermediate node I_i will record the ID of its upstream node for backward tracking and continue to rebroadcast the JREQ packet.

As a JREQ packet has arrived in one of the receivers R_i , it will conduct the similar process to wait for other JREQ packets for the Collection Time of the Receiving node (CT_R). R_i will select the path with the highest weight and initiate the transmission of a join reply (JREP) packet back to the source node S . While an intermediate node I_i receives the JREP packet, it will determine if it is on the reverse path towards S by verifying the next node ID in the JREP packet with its own ID. If the two IDs are identical, I_i will increment its node weighting (i.e. $I_i.N_WGHT++$) and continue to rebroadcast the JREP packet. On the other hand, the weighting will be decremented if I_i does not receive any JREP within the time interval specified in the N_WGHT Count Down Timeout (CDT) parameter. This process will be terminated until all the JREP packets have arrived in the source node S . The detail heuristic algorithm for constructing the routing structure is shown in Algorithm 3 and 4.

Within the proposed ECMR protocol, there is no additional control packet required for each node to depart from the existing structure \mathcal{T} . The source node S can terminate its periodic broadcast of the JREQ packets; while the receiving node R_i simply ceases the transmission of the JREP packet. Without receiving the JREP packet from R_i , the intermediate node I_i will also count down its weighting parameter ($I_i.N_WGHT$), which makes it become less important within the structure \mathcal{T} .

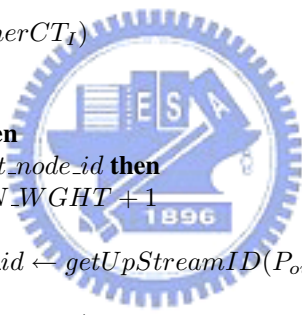
9.2 The Pseudo Code of Heuristic Structure Construction

The pseudo code of the heuristic algorithm for constructing the multicast routing structure \mathcal{T} is shown in Algorithm 1. This heuristic algorithm can be separated into three parts: procedures of the source node, procedures of the intermediate node, and procedures of the receiving node. In the procedures of the source node, the source node creates a JREQ packet (i.e. P_{new}) for every time period of FLDT,

Algorithm 3: Heuristic Structure Construction

Data:

```
1 Procedure of the Source Node begin
2    $round \leftarrow 0$ 
3   while true do
4      $round \leftarrow round + 1$ 
5      $P_{new} \leftarrow \text{new JREQ\_Packet}(ID_{source}, round)$ 
6      $\text{broadcast}(P_{new})$ 
7      $\text{waitTimeout}(FLDT)$ 
8   end
9 end
10 Procedure of the Intermediate Node begin
11    $\text{demoteMechanism} \leftarrow \{SLOW \text{ or } FAST\}$ 
12    $N\_WGHT \leftarrow 0$ 
13    $P_{best} \leftarrow null$ 
14   while true do
15      $P_{in} \leftarrow \text{getIncomingPacket}()$ 
16     if  $P_{in}.type = JREQ$  then
17       if  $P_{in}.round = P_{best}.round$  then
18         if  $P_{in}.P\_WGHT > P_{best}.P\_WGHT$  then  $P_{best} \leftarrow P_{in}$ 
19       end
20       if  $P_{in}.round > P_{best}.round$  then
21          $P_{best} \leftarrow P_{in}$ 
22          $\text{startTimer}(timerCT_I)$ 
23       end
24     end
25     if  $P_{in}.type = JREP$  then
26       if  $ID_{self} = P_{in}.next\_node\_id$  then
27          $N\_WGHT \leftarrow N\_WGHT + 1$ 
28          $P_{out} \leftarrow P_{in}$ 
29          $P_{out}.next\_node\_id \leftarrow \text{getUpStreamID}(P_{out})$ 
30          $\text{broadcast}(P_{out})$ 
31          $\text{stopTimer}(timerCDT)$ 
32       end
33     end
34     if  $\text{isExpired}(timerCT_I)$  then
35        $P_{best}.P\_WGHT \leftarrow P_{best}.P\_WGHT + N\_WGHT$ 
36        $\text{broadcast}(P_{best})$ 
37        $\text{startTimer}(timerCDT)$ 
38     end
39     if  $\text{isExpired}(timerCDT)$  then
40       if  $N\_WGHT \neq 0$  then
41         if  $\text{demoteMechanism} = SLOW$  then
42            $N\_WGHT \leftarrow N\_WGHT - 1$ 
43         else
44            $N\_WGHT \leftarrow 0$ 
45         end
46       end
47     end
48   end
49 end
```



Algorithm 4: Cont.

```
Procedure of the Receiving Node begin
  while true do
     $JREQset \leftarrow collectJREQwithin(CT_R)$ ;
     $choice \leftarrow JREQset.pktWithMaxP\_WGHT()$ ;
    if  $choice.itemCount() \neq 1$  then
      |  $P_{out} \leftarrow randomPickOneIn(choice)$ 
    else
      |  $P_{out} \leftarrow choice.pop()$ 
    end
     $P_{out.type} \leftarrow JREP$ ;
     $P_{out.next\_node\_id} \leftarrow getUpStreamID(P_{out})$ ;
     $broadcast(P_{out})$ ;
  end
end
```

and also uses a variable "round" to record the round index of the newly generated P_{new} . According to the round index, the node overhearing the JREQ packet can determine the freshness of this JREQ packet (i.e. the larger round index represents the higher degree of freshness). Finally, the source node broadcast the newly generated P_{new} to its neighbors. In the procedures of the intermediate node, the variable demote-Mechanism acts as the option of SLOW or FAST demotion of N_WGHT . If the value is SLOW, the N_WGHT parameter will decrease one after the CDT timer expires. On the other hand, if the value is set to be FAST, the N_WGHT parameter will directly become zero. It will be shown in the following section that the variable demote-Mechanism can affect the converging time of \mathcal{T} . As shown in Algorithm 3 and 4, the procedures of the source node mainly consist of four code sections which deal with the receiving JREQ packets, the receiving JREP packets, the expiration of the CTI timer, and the termination of the CDT timer. In the first code section, the intermediate node collects the JREQ packets for the time period of CTI, and decides the best collected JREQ packet according to the P_WGHT parameter and the round index. And then the third code section rebroadcasts the best collected JREQ packet (i.e. P_{best}) when the CTI timer expires. In the second code section, the incoming JREP packet whose $next_node_id$ is equal to the intermediate node ID will be rebroadcast with a new $next_node_id$ of the corresponding upstream node ID recorded during the JREQ dissemination phase. In fact, this code section models unicasting by broadcasting. Finally, the fourth code section handles the decrement of the N_WGHT when the CDT timer expires. In the

procedures of the receiving node, the receiving node collects JREQ packets within the time period of CTR, and determines the JREQ packet with maximum P_WGHT . If there are two or more JREQ packets with the same maximum P_WGHT value, the random selection of these JREQ packets is adopted. This selected JREQ packet will be properly updated and transformed into the JREP packet (i.e. P_{out}). In the end, P_{out} will be broadcast to the neighbors to finish the JREQ/JREP negotiation and complete the structure construction.

9.3 Data Packet Forwarding

When the structure \mathcal{T} is constructed, the source node \mathcal{S} directly broadcasts the data packets to its neighbor, and then the nodes overhearing the data packets rebroadcast these packets if their N_WGHT parameters are not zero. Eventually, the data packets will reach all receivers in \mathcal{R} and finish the multicast data packet forwarding.



Chapter 10

Performance Evaluation

10.1 The Software and Hardware Architectures

The software and hardware architectures utilized for practical implementation are shown in left schematic diagram of Fig. 10.1. On the top of the software architecture, the Performance Measurement Interface (PMI) is employed as the tool for collecting and recording the experimental results. The ARM Linux [10] with version 2.4.19 is adopted as the Operating System (OS), which handles the inserted software modules (i.e. the so-called kernel modules) with mutual interaction. The three major kernel modules that are incorporated into the ARM Linux include the Socket Interface, the Netfilter, and the WLAN Driver. Moreover, the proposed ECMR protocol is implemented as a kernel module within the OS.

The Socket Interface provides a general operating interface of the transport layer, which supports both the TCP and the UDP packet transmissions. The ECMR algorithm utilizes the Socket Interface for creating and sending packets via the UDP transmission. It is noted that the UDP packet is utilized within the implementation due to its connection-less nature. Moreover, the Netfilter module [11] is adopted by the proposed ECMR protocol for packet-filtering. The Netfilter module consists of five hooks with the hook-specific events that are defined for IPv4 in the Linux header file, i.e. `<linux/netfilter.h>`. Each hook and the corresponding hook function can be triggered while the hook-specific event occurs. Moreover, the hook function will return either the `NF_DROP` or the

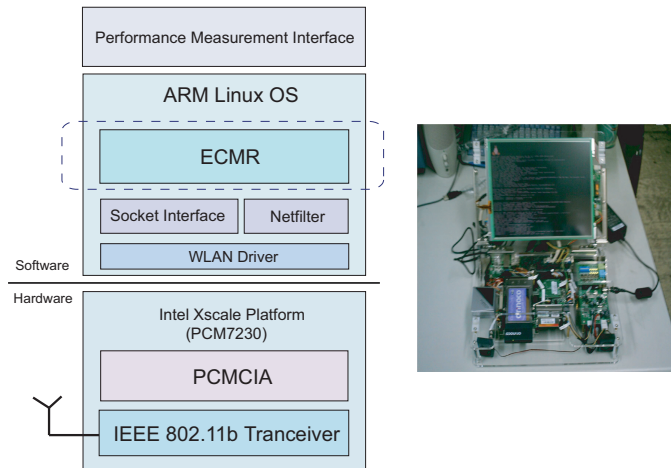


Figure 10.1: Left: the software and hardware architectures for the proposed ECMR protocol; Right: the snapshot of the PCM-7230 ARM-based embedded platform

NF_ACCEPT status code in order to either discard or facilitate the packet to pass through the hook. The NF_IP_PRE_ROUTING and the NF_IP_LOCAL_OUT correspond to the two hooks that are involved in the design of the ECMR scheme for manipulating both the incoming and the outgoing packets. The NF_IP_PRE_ROUTING hook is triggered as a packet is newly received from the wireless medium; while the NF_IP_LOCAL_OUT hook is initiated as an outgoing packet is generated. At the bottom of the software architecture, the WLAN driver is served as the communication bridge between the software packet control and the physical hardware transmission. The *wlan_cs* driver adopted in the implementation is available under the GNU General Public License (GPL).

Considering the hardware aspect, the PCM-7230 embedded platform [12] is shown in the right diagram of Fig. 10.1. It is an integrated embedded platform with an Intel XScal PXA-255 400MHz CPU, a PCMCIA interface, and other peripherals. It is noted that the PCM-7230 platform fulfills the essential hardware requirements for the design of the ECMR protocol. Moreover, the Lucent Orinoco WLAN card, which supports the IEEE 802.11b via the PCMCIA interface, is utilized as the wireless interface for packet transmission.

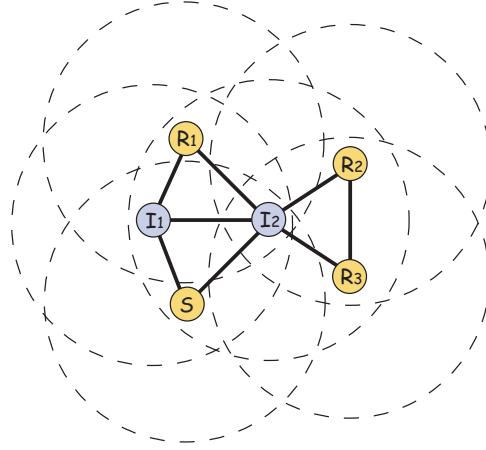


Figure 10.2: The network topology for field experiments: the source node S communicates with three receivers R_1 , R_2 , and R_3 via the intermediate nodes I_1 and I_2 . The solid lines denote the connectivity between the corresponding two nodes.

10.2 The Experiment Results

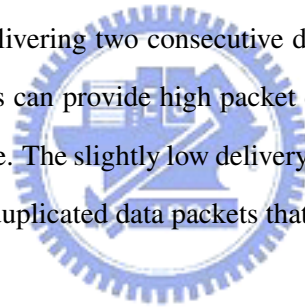
Field experiments are conducted in order to evaluate the performance of the proposed ECMR protocol. The ODMRP algorithm [5] is also implemented for comparison purpose. The network topology utilized in the experiments is illustrated as in Fig. 10.2. The source node S intends to deliver data packets to its corresponding receivers R_1 , R_2 , and R_3 via the intermediate nodes I_1 and I_2 . Two metrics are employed for performance comparison: the energy consumption for relaying data packets and the packet delivery ratio.

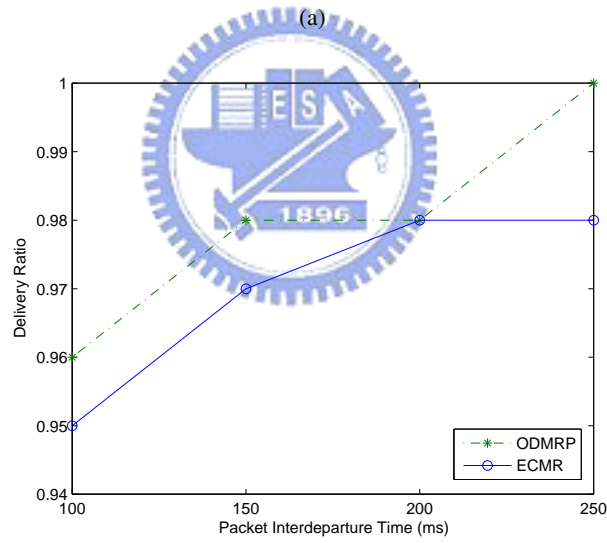
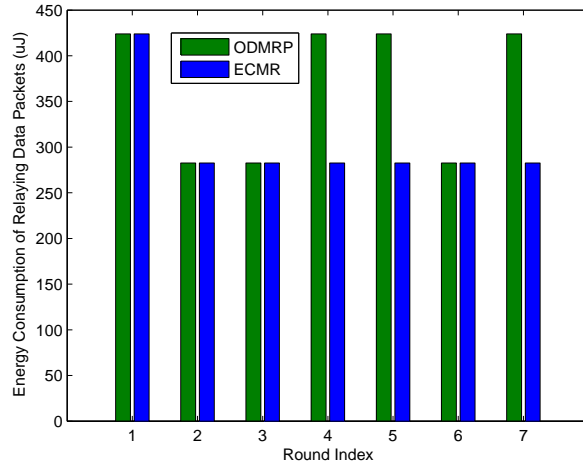
Fig. 10.3(a) shows the performance comparison between the ECMR and the ODMRP algorithms by observing the energy consumption versus the round index. It is noted that the round index represents each periodically refreshed round conducted by the route updating process. The energy consumption for relaying data packets is calculated by multiplying the total data packets delivered between every two rounds with the energy consumption for each packet transmission. It is noted that the transmitter bit rate equals 11 Mbps; while the transmitting power is 15 dBm. The data rate is fixed to 6 packets per round with each packet size of 1024 bytes. The parameters utilized within the ECMR protocol are listed as follows: FLDT = 6 sec, CDT = 0.5 sec, $CT_I = 1.5$ ms, and $CT_R = 30$ ms.

Since the ODMRP protocol is designed based on the shortest path construction, node R_1 will randomly select either I_1 or I_2 as its upstream node. Moreover, I_2 is consistently chosen since it is the

only node on the shortest path to both R_2 and R_3 . Consequently, the number of required intermediate nodes by adopting the ODMRP algorithm will alternate between one and two, which results in the fluctuation on the energy consumption versus the round index (i.e. the green bars as shown in Fig. 10.3(a)). On the other hand, the number of intermediate nodes will always be one after the second round by exploiting the proposed ECMR protocol. Considering the worst case, node R_1 will select I_1 as the upstream node to S in the first round. In the remaining rounds, node R_1 will always select I_2 as the upstream node to S since the N_WGHT parameter from node I_2 is greater than that from node I_1 . It can be seen from the experimental results (in Fig. 10.3(a)) that the energy consumption by using the ECMR protocol is comparably less than that from the ODMRP algorithm. It is also noticed that as the available number of intermediate nodes is increased, the benefits of adopting the ECMR algorithm will become more observable.

Fig. 10.3(b) shows performance comparison considering the packet delivery ratio versus the interdeparture time (with packet size of 1024 bytes). It is noted that the packet interdeparture time represents the time interval for delivering two consecutive data packets. It can be seen that both the ECMR and the ODMRP protocols can provide high packet delivery ratio (with almost 100%) under different packet interdeparture time. The slightly low delivery ratio resulted from the ECMR algorithm is attributed to its less number of duplicated data packets that are transmitted.





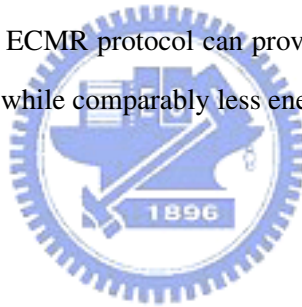
(b)

Figure 10.3: (a) Energy Consumption for Relaying Data Packets vs. Round Index, (b) Packet Delivery Ratio vs. Packet Inter-Departure Time.

Chapter 11

Conclusion

An Energy-Conserving Multicast Routing (ECMR) protocol for the wireless multihop networks is proposed in this paper. Both the proposed ECMR protocol and the existing mesh-based ODMRP algorithm are implemented on an ARM-based embedded platform for performance evaluation. The experimental results show that the ECMR protocol can provide high packet delivery ratio under different packet inter-departure time; while comparably less energy is consumed.



Bibliography

- [1] E.M. Royer and C.E. Perkins, "Multicast Operation of the Ad-Hoc On-Demand Distance Vector Routing Protocol," *Proc. of the Fifth Annual ACM/IEEE International Conference on Mobile Computing and Networking*, pp. 207-218, Aug. 1999.
- [2] C.W. Wu and Y.C. Tay, "AMRIS: A Multicast Protocol for Ad Hoc Wireless Networks," *Proc. of IEEE Military Communications Conference*, Vol. 1, pp. 25-29, Oct. -Nov. 1999.
- [3] J. Xie, R.R. Talpade, A. Mcauley, and M. Liu, "AMRoute: Ad Hoc Multicast Routing Protocol," *ACM/Kluwer Journal of Mobile Networks and Applications*, Vol. 7, Iss. 6, pp. 429-439, Dec. 2002.
- [4] S.K.S. Gupta and P.K. Srimani, "An Adaptive Protocol for Reliable Multicast in Mobile Multi-Hop Radio Networks," *Proc. of the Second IEEE Workshop on Mobile Computing Systems and Applications*, pp. 111-122, Feb. 1999.
- [5] S.J. Lee, M. Gerla, and C.C. Chiang, "On-Demand Multicast Routing Protocol," *Proc. of IEEE Wireless Communications and Networking*, Vol. 3, pp. 1298-1302, Sept. 1999.
- [6] S.J. Lee, W. Su, and M. Gerla, "On-Demand Multicast Routing Protocol in Multihop Wireless Mobile Networks," *ACM/Kluwer of Mobile Networks and Applications*, Vol. 7, pp. 441-453, Dec. 2002.
- [7] J.J. Garcia-Luna-Aceves and E.L. Madruga, "The Core-Assisted Mesh Protocol," *IEEE Journal on Selected Areas in Communications*, Vol. 17, Iss. 8, pp. 1380-1394, Aug. 1999.

- [8] P. Sinha, R. Sivakumar, and V. Bharghavan, "MCEDAR: Multicast Core-Extraction Distributed Ad Hoc Routing," *IEEE Wireless Communications and Networking Conference*, Vol. 3, pp. 1313-1317, Sept. 1999.
- [9] P.M. Ruiz and A.F. Gomez-Skarmeta, "Approximating Optimal Multicast Trees in Wireless Multihop Networks," *Proc. of IEEE Computers and Communications (ISCC)*, pp. 686-691, Jun. 2005.
- [10] Wookey and Tak-Shing, "Porting the Linux Kernel to a New ARM Platform," *Wireless Solutions Journal*, Vol. 4, pp. 52-59, 2002.
- [11] K. Wehrle, F. Pählke, Hartmut, D. Müller, and M. Bechler, "The Linux Networking Architecture: Design and Implementation of Network Protocols in the Linux Kernel," *Prentice Hall*, Aug. 2004.
- [12] "PCM-7230 User's Manual," *Advantech Co., Ltd.*, 2003.

